APPLICATION OF A FREQUENCY APPROACH TO THE
CLASSIFICATION OF ELECTROCARDIOGRAPH SIGNALS

by

PAUL JOSEPH MILNE

B.S., Worcester Polytechnic Institute, 1967

9589

_____

A MASTER'S THESIS

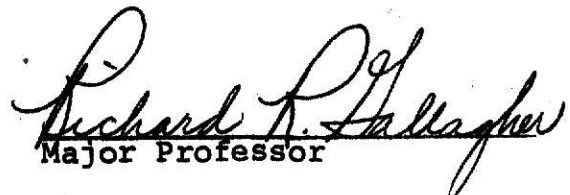submitted in partial fulfillment of the

requirements for the degree

MASTER OF SCIENCE

Department of Electrical Engineering

KANSAS STATE UNIVERSITY
Manhattan, Kansas

1972

Approved by:

Major Professor

TABLE OF CONTENTS

INTRODUCTION

Many advances in the application of electronics to medicine have been made in recent years. Devices for the measurement and modeling of physiological events have enhanced the understanding of the events studied. The computer has also played a very important role in the rapid processing of physiological data.

A computer can be programmed to perform a given analysis of physiological data and to arrive at a conclusion which in many cases would be a suggested diagnosis. To do this the computer must be programmed such that it makes use of the vast amount of past medical experience.

The electrocardiographic signal is one type of physiological data which can be analyzed using a digital computer. Before the computer can be used to analyze the ECG, the ECG data must be put into the appropriate digital (i.e., sampled) form. Fig. (1-1) The sampled data is then used to represent the continuous ECG signal.

Computer analysis of ECG's is usually carried out in two steps. The first step involves a pattern recognition program which extracts features associated with the ECG signal which are used to identify it as a normal or an abnormal ECG. The second step involves the use of a program which uses these features to classify an ECG as belonging to the normal or abnormal class.

There are basically three approaches to the solution of the above problem. These are: (i) time-domain approach, (ii) cross-correlation approach, and (iii) frequency analysis approach.
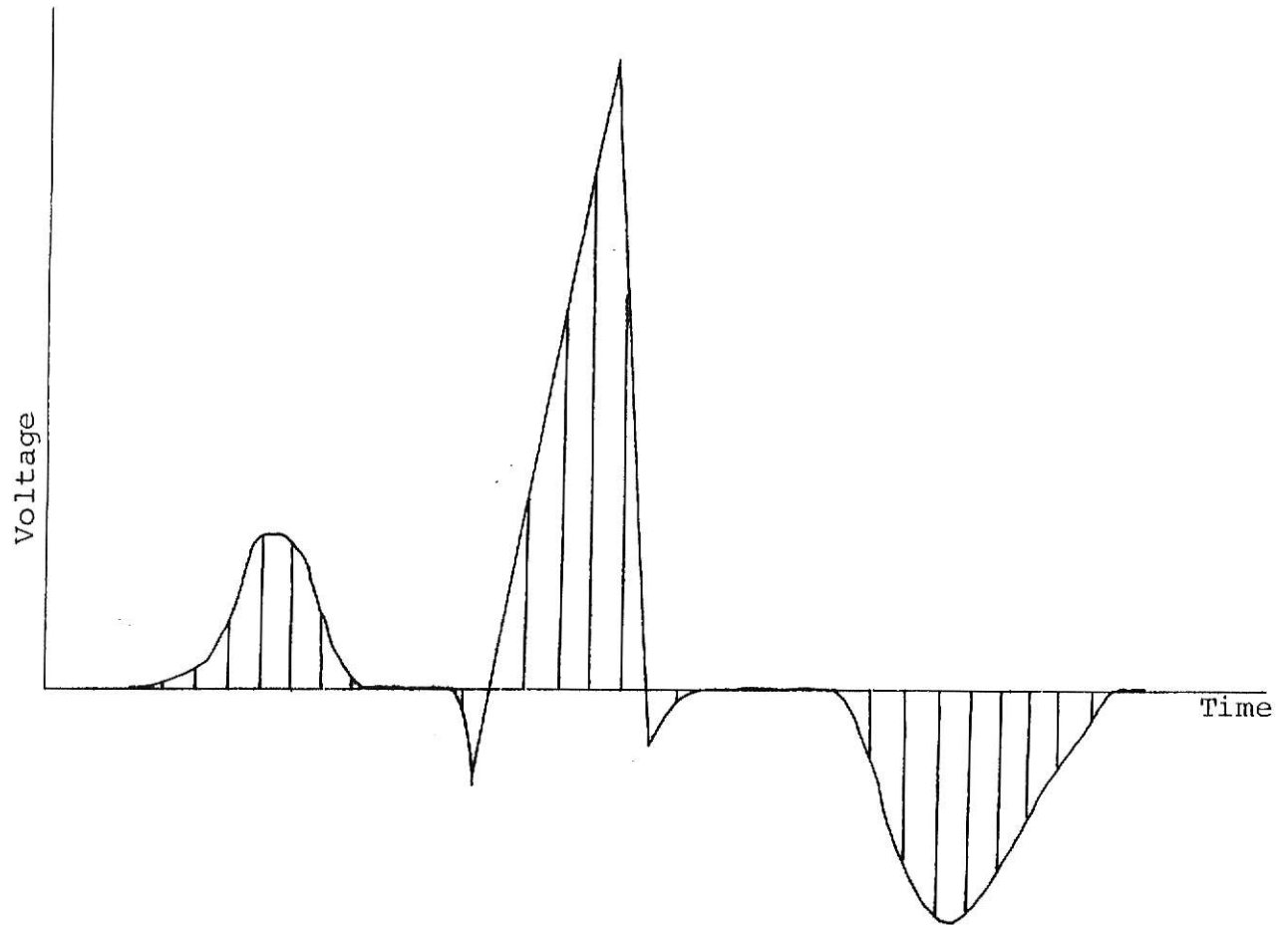
Fig. 1-1. Sampled form of ECG.

i. Time Domain Approach

The time domain approach uses features similar to those that the cardiologist uses to distinguish a normal ECG from an abnormal ECG. The steps involved in this process include [40]:

1. location of the QRS complex

2. QRS envelope pattern determination

3. recognition of the T wave and the S-T segment, and

4. detection of the P wave.

This approach is called the "time domain approach" since the ECG signal (which is a function of time) is processed directly to extract the desired features.

ii. Cross Correlation Approach

In this approach the incoming ECG signal is cross correlated with standard ECG patterns whose classifications are known. The classification is made on the basis of the degree of correlation between the incoming signal and the known signals. The pattern with the highest correlation to the incoming signal is chosen. Cross correlation represents the degree to which two patterns or signals represent each other. The cross correlation of two identical signals would be unity.

iii. Frequency Analysis Approach.

In this approach the ECG is represented in terms of a class of functions consisting of the Fourier and Walsh Functions [4]. These functions characterize the ECG by their ability to show the distribution of power in the ECG signal.

Much previous work has been done using the time domain approach [34,36]. This approach, however, has disadvantages associated with measuring the various time intervals of the ECG and automatically recognizing the different segments of the ECG. The programs usually used for the time domain analysis are usually cumbersome and require a special purpose or general purpose computer to implement.

Relatively little has been reported using the cross correlation approach or the frequency approach. The difficulties that the cardiologst encounters when attempting to interpret the significance of the frequency domain signal characteristics contributes to this fact. For example, an ECG characteristic such as notching in the time domain signal is easier to evaluate than a correlation coefficient or frequency component.

In this study the frequency domain approach was investigated. Canine ECG signals were used and were classified as normal or abnormal by a trained cardiologist. The Bifore (Binary Fourier Representation) was used to characterize the ECG signal [4]. The features obtained from the ECGs using the Bifore power spectrum were then used to train a classifier. The trained classifier was then used to classify unknown ECG signals as normal or abnormal.

This study, it is hoped, has shown that the frequency domain and the Bifore power spectrum can be used successfully in the analysis of electrocardiographic data.

II

TERMINOLOGY

1. [43] An <u>algorithm</u> is a rule for computation.

2. [38] An <u>arrythmia</u> is an irregular heart action causing the absence of rhythm.

3. [38] The <u>atrium</u> is one of the upper chambers of the heart.

4. [4] An <u>augmented pattern vector</u> is obtained from a d-dimensional pattern vector by adding a (d+1) st. component equal to -1.

5. [4] <u>Bifore</u> - <u>B</u>inary <u>F</u>ourier <u>R</u>epresentation

6. [4] The <u>confusion matrix</u> is a summary of the results of the classification process. The off diagonal terms indicate errors made in classification.

7. [43] <u>Correlation</u> is a measure of the degree of relationship between two signals.

8. [4] <u>Decision numbers</u> are the numbers used in the classification process derived from the training set.

9. [38] <u>Depolarization</u> is the reduction of the potential across a membrane with respect to the resting membrane potential.

10. [4] <u>DFT</u> - <u>D</u>iscrete <u>F</u>ourier <u>T</u>ransform

11. [43] <u>Distortion</u> is error in representation. In signal processing this error is seen in the waveform characteristics being analyzed.

12. [38] The <u>electrocardiograph</u> signal ECG, is the record of the electrical activity of the heart measured on the body surface.

13. [38] An <u>electrolyte</u> is a substance which in solution con-
ducts an electric current.

14. [4] The <u>FBT</u> or <u>F</u>ast <u>B</u>ifore <u>T</u>ransform is an algorithm for
the computation of the Bifore Transform.

15. [4] The <u>FFT</u> or <u>F</u>ast <u>F</u>ourier <u>T</u>ransform is an algorithm for
the computation of the Discrete Fourier Transform.

16. [4] The <u>frequency response</u> of a system is a measure of its
reaction to signals with different rates of variation.

17. [38] <u>Hypertrophy</u> is the increase in size of an organ or of
a structure.

18. [38] An <u>infarct</u> is an area of tissue in an organ or part
which undergoes necrosis following cessation of blood
supply.

19. [38] <u>Ischemia</u> is local and temporary anemia due to obstruc-
tion of circulation to segments of the body.

20. [43] An <u>iteration</u> is a step of a repeated procedure.

21. [22] A <u>lead system</u> refers to a well defined method for
positioning of electrodes on the surface of the body
for recording of the ECG.

22. [4] The <u>method of least squares</u> is a method of arriving
at a mean value in such a way that the mean of the
error squared is minimized.

23. [14] <u>Mass screening</u> refers to the testing of large numbers
of individuals for ECG abnormalities.

24. [38] The <u>membrane resting potential</u> is the potential across
a membrane in the absence of electrical activity.

25. [38] Metabolism refers to energy and material transforma-
         tions occurring in living cells.

26. [4]   A mode consists of a group of characteristics belong-
         ing to the same category.

27. [38] Myocardial refers to the muscle of the heart.

28. [38] Myocardium - the heart muscle.

29. [43] Orthogonality is the property of having a rectangular
         coordinate system.

30. [4]   A pattern vector is a vector composed of numbers de-
         rives from the characteristics of a given signal.

31. [38] Pericarditis is the inflammation of the pericardium,
         or heart sac.

32. [4]   The power spectrum is a measure of the energy content
         in different portions of the frequency domain.

33. [38] Repolarization is the process by which the membrane
         returns to its resting potential after being depola-
         rized.

34. [21] Serial electrocardiography is the system of recording
         a subject's ECG for comparison to ECGs to be taken at
         a later time. It is valuable in detecting changes in
         an individual's ECG.

35. [4]   Shift Invariance is the property of periodic signals
         which states that a given shift invariant measurement
         is unaffected by the point in the signal where the
         measurements begin.

36. [38] <u>Systemic</u> refers to the blood flow from the left ventricle through the arteries, arterioles, capillaries, venules, and venous system which empties into the right atrium.

37. [4] A <u>threshold unit</u> is a detection device which switches from one state to another when a preset value is reached.

38. [4] A <u>training set</u> is a group of known signals used to generate the decision numbers of a classifier.

39. [43] A <u>transform</u> is a mathematical method of changing one representation of a signal to another.

40. [38] The <u>ventricles</u> are the pumping chambers of the heart. The left ventricle pumps into the aorta and the right vectricle pumps into the pulmonary artery.

III

INTRODUCTION TO ELECTROCARDIOGRAPHY

3.1 Membrane Potential

The electrocardiogram is an indication of the electrical events taking place in the myocardium. The electric potential is generated by the depolarization and repolarization of the muscle cells. Contraction of muscle mass is a consequence of the depolarization of the muscle cell membrane. In non-contracting muscle cells there is a potential gradient due to the greater concentration of positive ions outside of the cell as compared to inside of the cell. The potential so developed is called the membrane resting potential and is approximately -90 mv. This potential is primarily due to the ionic gradient. The depolarization of the cell membrane to both sodium and potassium ions Movement of sodium ions into the cell and the potassium ions out of the cell results in the membrane potential increasing to approximately +20 mv. A simplified explanation of muscle repolarization is the following: the sodium and potassium ions return to their original concentrations inside and outside of the cell resulting in the return of the membrane resting potential. Fig. (3-1) shows this sequence of events for a single ventricular muscle cell. Again, the electrocardiogram is the electric signal measured at the body surface, and represents the depolarization and repolarization of the myocardium tissue.
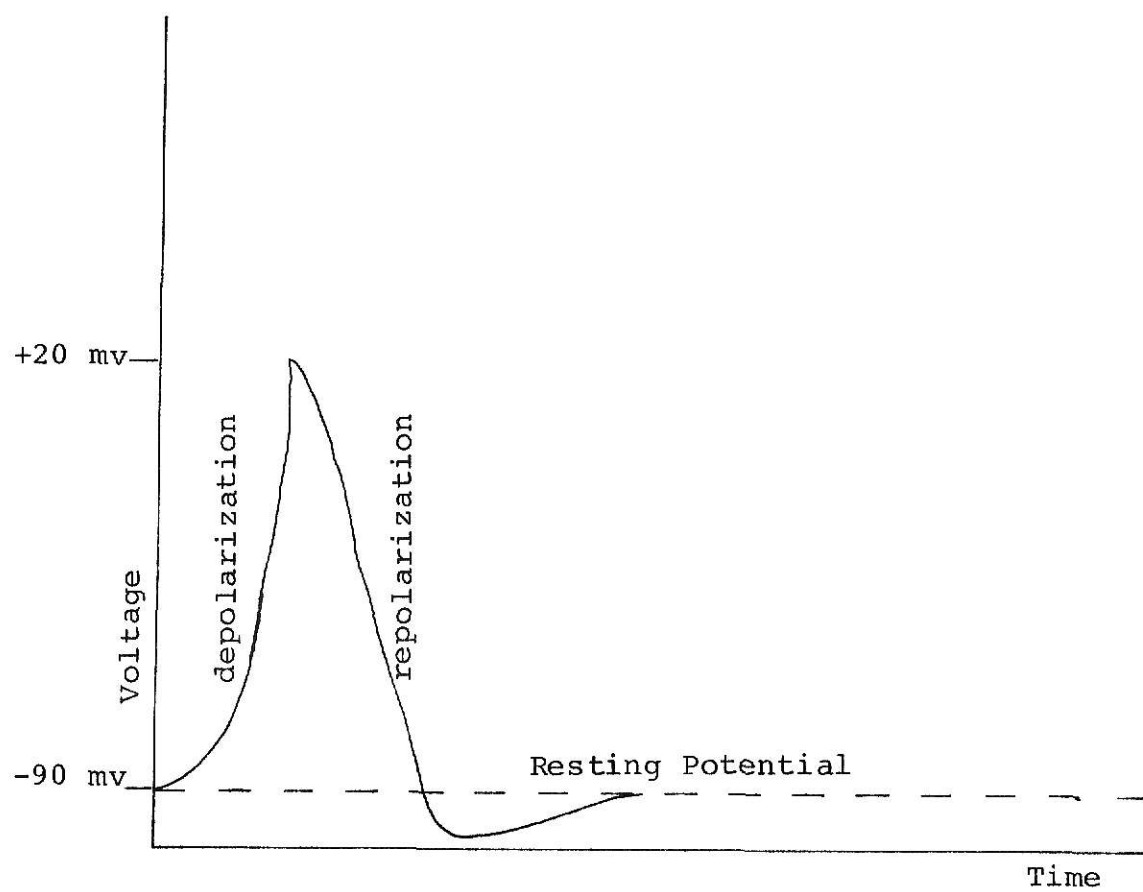
Fig. 3-1. Depolarization and repolarization
of a muscle cell.

3.2 Overview of Circulatory System

The heart is a cyclic pump, that is, there are events which cycle each time that the heart pumps blood to the body. In tracing a *drop* of blood through the circulatory system, the following events would be encountered. Blood enters the right atrium of the heart from the vena cava. Generally speaking this blood is deficient in oxygen and heavily laden with carbon dioxide. Contraction of the right atrium forces the blood through the tricuspid valve into the right ventricle. The right ventricle aids the passage of the blood through the semilunar valve into the pulmonary artery which carries it to the lungs. The capillary system of the lungs provides for the exchange of carbon dioxide for oxygen. The oxygenated blood then travels to the left atrium via the pulmonary vein. The left atrium again contracts and the blood enters the left ventricle through the mitral valve. Here it should be noted that the left and right chambers of the heart function almost simultaneously. When the ventricles contract, the blood is pumped out of the left ventricle into the aorta from whenc it is distributed to the body by the arterial system. After passin through the arterial and capillary systems the blood again enters the venous system and the cycle is repeated.

3.3 Generation of ECG Signal

The electrocardiograph signal shows the sequence of events of this heart cycle. The initiating pulse is generated in the sino-atrial node and triggers the depolarization and contraction of the atria. This depolarization is shown as the "P" segment of the ECG. The bioelectric signal then travels to the atrio-

ventricular node where it is slowed down before being transmitted to the ventricles. The impulse is transmitted first to the Bundle of His, a group of special conducting nerve fibers which "short circuit" the triggering pulse to the apex of the heart. While the ventricles are contracting the atria are repolarizing or returning to their resting potential. The repolarization of the atria which occurs approximately at the initial phase of the depolarization of the ventricles is masked by the latter event due to the relatively large muscle masses of the ventricles as compared to the atria. The depolarization of the ventricles is shown in the "QRS" segment of the ECG. After this depolarization and contractio of the ventricles they repolarize to return to their resting potential. The repolarization of the ventricles begins at the apex of the heart and travels towards the base. This repolarization manifests itself as the "T" segment of the ECG. Figure (3-2) illustrates this process.

3.5 Recording the ECG

There are several different accepted lead systems used to record the ECG. The one most commonly used is the so-called standard lead system. This system consists of three leads or pairs of connections. Its configuration is that shown in Fig. (3-3). Another useful lead system is the orthogonal lead system. This system measures the heart's electrical activity in three dimensions. Its advantage is that these three dimensions are nearly orthogonal to each other yielding a maximum amount of information about the ECG and the corresponding electrical
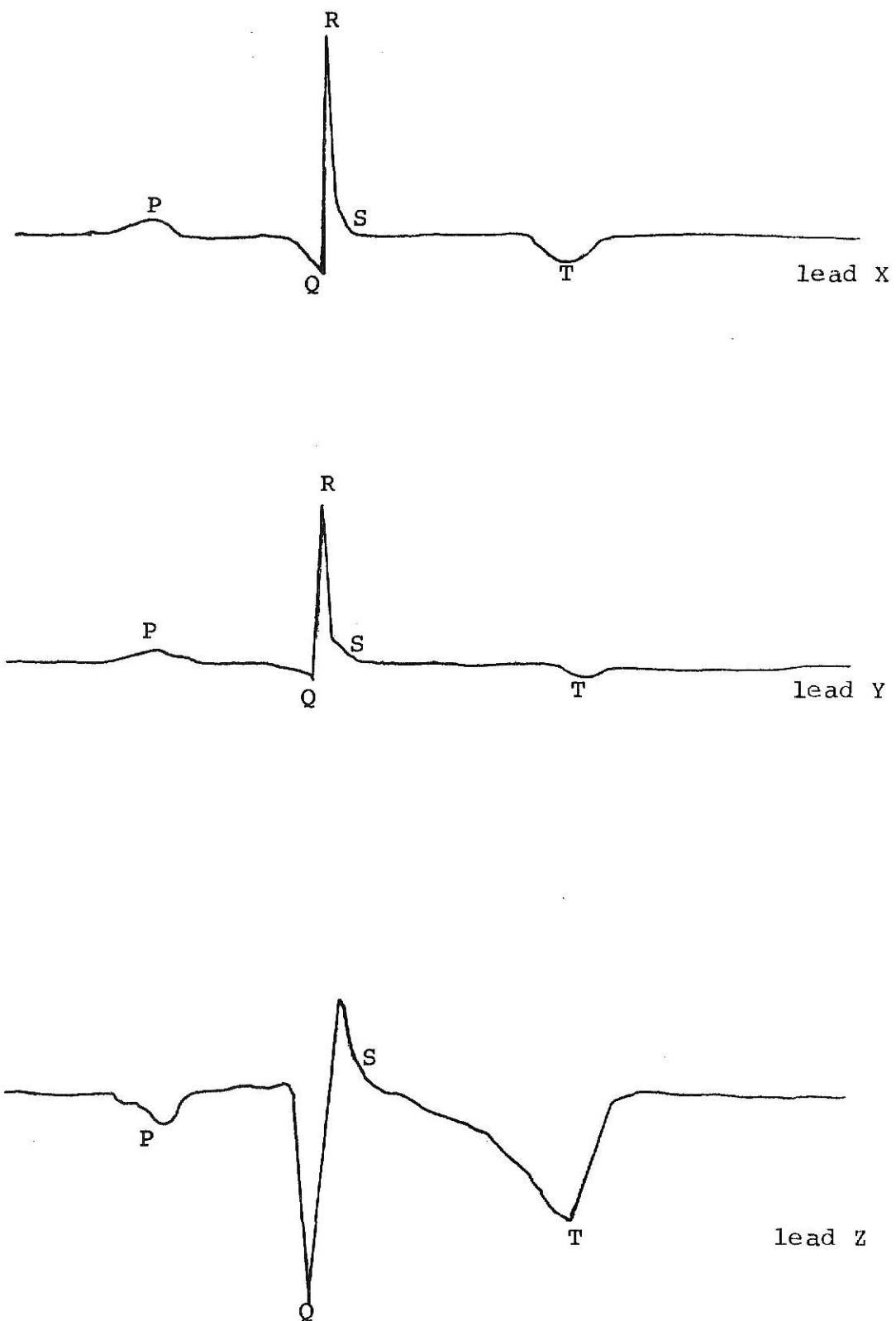
Fig. 3-2. ECG waveforms obtained
using X Y Z lead system.

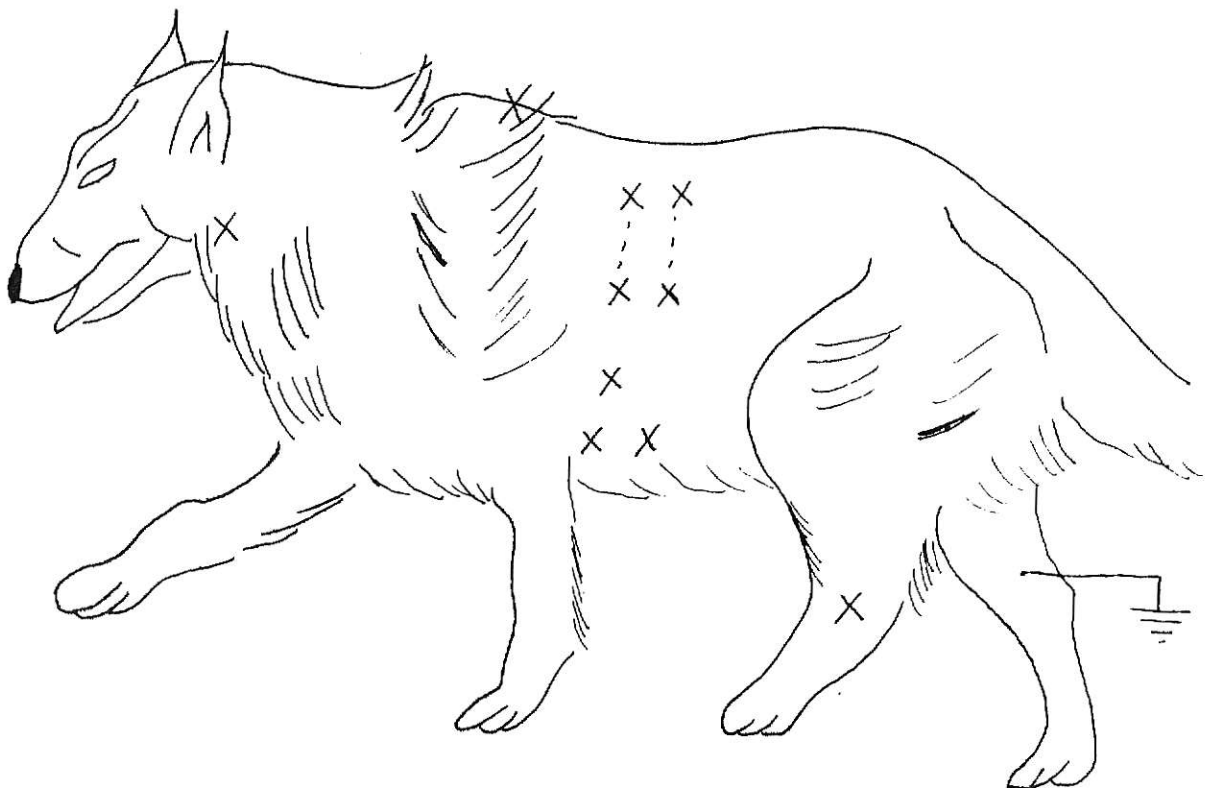Fig. 3-3. The Standard Lead System Configuration.

Fig. 3-4. The X Y Z Lead System Configuration.

activity of the heart. Figure (3-4) shows the McFee orthogonal XYZ lead system configuration used in this study.

3.6 Diagnostic Significance of ECG

The information obtained from the ECG is useful in the diagnosis of the following conditions [20]:

A. Atrial and ventricular hypertrophy

B. Myocardial infarction

C. Arrhythmias

D. Pericarditis

E. Systemic diseases affecting the heart

F. Effect of cardiac drugs on the heart

G. Disturbances in the electrolyte metabolism

In observing an ECG the given signal is compared to a normal signal. It would be very easy to diagnose any of the above conditions if a normal signal meant that only one possible waveform was present. This is not the case. The normal ECG signal consists of a range of signals. Both the period and the amplitude of the normal signal may vary within limits, with the signal being classified as normal. Even the shape of the waveform may vary among healthy subjects. Such factors as the orientation of the heart and the physical size of the subject may cause the ECG to vary from that of the so-called normal. This variation must be kept in mind when trying to analyze the ECG to ascertain the condition of the subject's heart. For a complete diagnosis of cardiac abnormalities information in addition to the ECG is utilize
The ECG, however, is probably the most significant.
References: [14,18,22,35,40].

IV

LITERATURE SEARCH

4.1 Frequency Response of ECG Monitoring System

The development of a system to automate electrocardiographic data analysis is dependent upon the choice of a suitable set of specifications for the system. In electrocardiography, one of the most important specifications for the system to be used is that of its frequency response.

Berson and Pipberger [8] studied the low frequency response needed for accurate reproduction of the ECG. In that study, it was shown that errors due to inadequate low frequency response were evidenced in distortions in the S-T segment and the T wave. These segments and the T wave are important in recognizing acute myocardial infarctions, myocardial ischemia, the effects of exercise and many other conditions. Eleven abnormal and twenty four normal ECGs were studied. It was found that the abnormal waveforms were more readily distorted due to inadequate low frequency characteristics of the recording system than the normal waveforms. It was suggested that low frequency characteristics of a 3 db. cutoff frequency at .05 Hz. and 6 db. per octave roll off would give better accuracy and that this increased accuracy would be desirable with the advent of better recording systems and the introduction of computer analysis.

In a later study Berson and Pipberger [7] studied the effects of inadequate high frequency response of recording devices. It was found that the QRS complex is the most affected part of the

ECG when the recording device does not have sufficient high frequency characteristics. The amplitude characteristics of the QRS complex were found to be directly related to the high frequency response characteristics of the recording device, while the QRS time durations were affected relatively little by its high frequency performance. Both normal and abnormal records were similarly affected. It was suggested that in order to reduce the QRS amplitude errors to less than .10 mv a 3 db. cutoff frequency greater than 100 Hz. was required. To reduce these errors to below .05 mv a 3 db. cutoff frequency greater than 200 Hz. was suggested.

Scher and Young [34] suggested that the contributions by frequencies greater than 100 Hz. are less than ten per cent of the amplitude of the fundamental component of the QRS complex.

Langner and Geselowitz [25] also studied the high frequency characteristics of the ECG. In that study it was found that in post-coronary subjects there was increased notching and slurring in the ECG. These effects increase the high frequency energy of the ECG. Substantial 1000 Hz. components were often observed and it was suggested that a system with a frequency response of 500 Hz. - 1000 Hz. would be adequate to record most of the high frequency information contained in the ECG. Although the high frequency components may be less than ten per cent of the amplitude of the original waveform, these high frequency components may be of great clinical value in diagnosis. Franke et al [19] also supported the importance of these high frequency components in diagnosis.

4.2 Sampling Rate and Leads Necessary for Reproduction of the ECG

In a paper discussing the use of computers in analyzing ECG data, Pipberger [30] pointed out several observations in the use of the computer in electrocardiography. It was found that a high sampling rate is desired for numerical reproduction of the ECG. This study found that a three lead system is sufficient for computer ECG analysis and that a set of spatial ECG measurements proved to be superior to those measurements obtained from a scalar lead system.

4.3 Systems in Use

Whiteman et al reported on an automated system used for more than two years in processing over 50,000 twelve lead ECGs [41]. The processing consisted of three steps. The first step was to condense the data and to pick out the most significant data for diagnosis. The second step was that of combining the data. It was necessary to combine these data in such a way that a given combination would show a particular abnormality. The third and final step was that of diagnosis. The most general diagnosis was used. For example, if the criteria for two abnormalities were met but one was contained in the other, the most general category would be chosen as the diagnosis. It was also emphasized that the computer was to aid the physician and to call his attention to possible conditions of abnormality, but that the physician was the ultimate decision maker.

Cooper et al [16] used the digital computer analysis of ECGs in a community health department. It was felt that the

computer would fill the need of such an organization since rapid,
low-cost medical diagnostic procedures were needed. The ECGs
were recorded during the day and then sent to a computing center
in the evening for interpretation. The results were classified
as normal, minor abnormal, and major abnormal. The patients in
the third class and their physicians were notified. The patient's
physicians in the second class were also notified. In addition,
this computer analysis was used successfully in routine screen-
ing and in home care.

4.4 Time Domain Approach

Most of the applications of computers to electrocardiography
have involved studying the ECG in the time domain [5-16,18,28-33,
36,37,41]. The procedures used include the measurement of slope,
amplitude and time intervals within and for the complete ECG.
The computer is then programmed to recognize these characteris-
tics in much the same way that a cardiologist intreprets the ECG
recording. A range of acceptable characteristics is developed
and then used as a basis for classification of the ECG signal.
One of the most difficult problems in the above time domain
approach encountered was that of recognizing the different seg-
ments of the ECG [40,42]. The QRS complex seemed to provide the
most accurate reference point in determining which point of the
ECG was being sampled. The positive and negative slopes of this
complex were the most often used characteristics for identifica-
tion of this segment of the ECG.

4.5 Defining the Range of Normal ECGs

Another difficulty encountered in the classification of ECGs is that of defining the range of normal for ECGs. Wartak [40] pointed out that the normal values of the ECG components are usually obtained by the statistical analysis of the data from a large number of normal individuals. A normal subject was defined as one who has been in the past and is presently free from overt cardiovascular diseases or any condition which frequently results in some form of cardiovascular disease. The statistical distribution of most normal ECG parameters was found to be skewed to the right. In the case of this asymmetrical distribution, it was suggested that the limits of normal be defined using the ninety-six percentile range with two per cent eliminated from both the minimal and maximal ends of the distribution. If the ECG parameter in question does have a normal (symmetrical) distribution, it was suggested that the range of normal be defined as the mean plus or minus two standard deviations to include ninety-five per cent of this normal population.

Graybiel et al [21] studied the ECGs obtained from 100 young, healthy aviators with a mean age of 23.7 years. It was shown that there is a considerable overlap between the normal and abnormal range for the ECG . After noting the great variation between normal ECGs, it was suggested that serial electrocardiography would be of great value to the physician in detecting a subject's change in ECG.

V

THE FREQUENCY APPROACH

To classify a given ECG signal its signature must be ascertained. A signature is a group of features or attributes which serve to distinguish a normal ECG from one that is abnormal. The signature used in this study for the classification of normal and abnormal ECGs is that of the power spectral points of the signal's Bifore transform.

The BT transforms the time domain signal into the frequency domain. It belongs to a family of transforms which are known as orthogonal transforms. Such transforms have a unique property in that they yield the distribution of power (i.e. the rate of change of energy) in an ECG signal. Such distributions are used as signatures to help determine the classification of an incoming ECG. A brief description of two members of this family of orthogonal transforms follows. A more complete description of these transforms is available in references [2-4].

5.1 Discrete Fourier Transform (DFT)

Definition:

Let $[X(m)]$, $m=0,1,\ldots,(N-1)$ denote a sequence of N-periodic real numbers obtained by sampling an ECG signal as shown in Fig. (5-1). The DFT corresponding to the ECG is defined as

$$C_x(k) = \frac{1}{N} \sum_{m=0}^{N-1} X(m) W^{km}, \quad k=0,1,\ldots,(N-1) \tag{5-1}$$

where $W = e^{-i\frac{2\pi}{N}}$, $i = \sqrt{-1}$ and the $C_x(k)$ are the DFT coefficients.
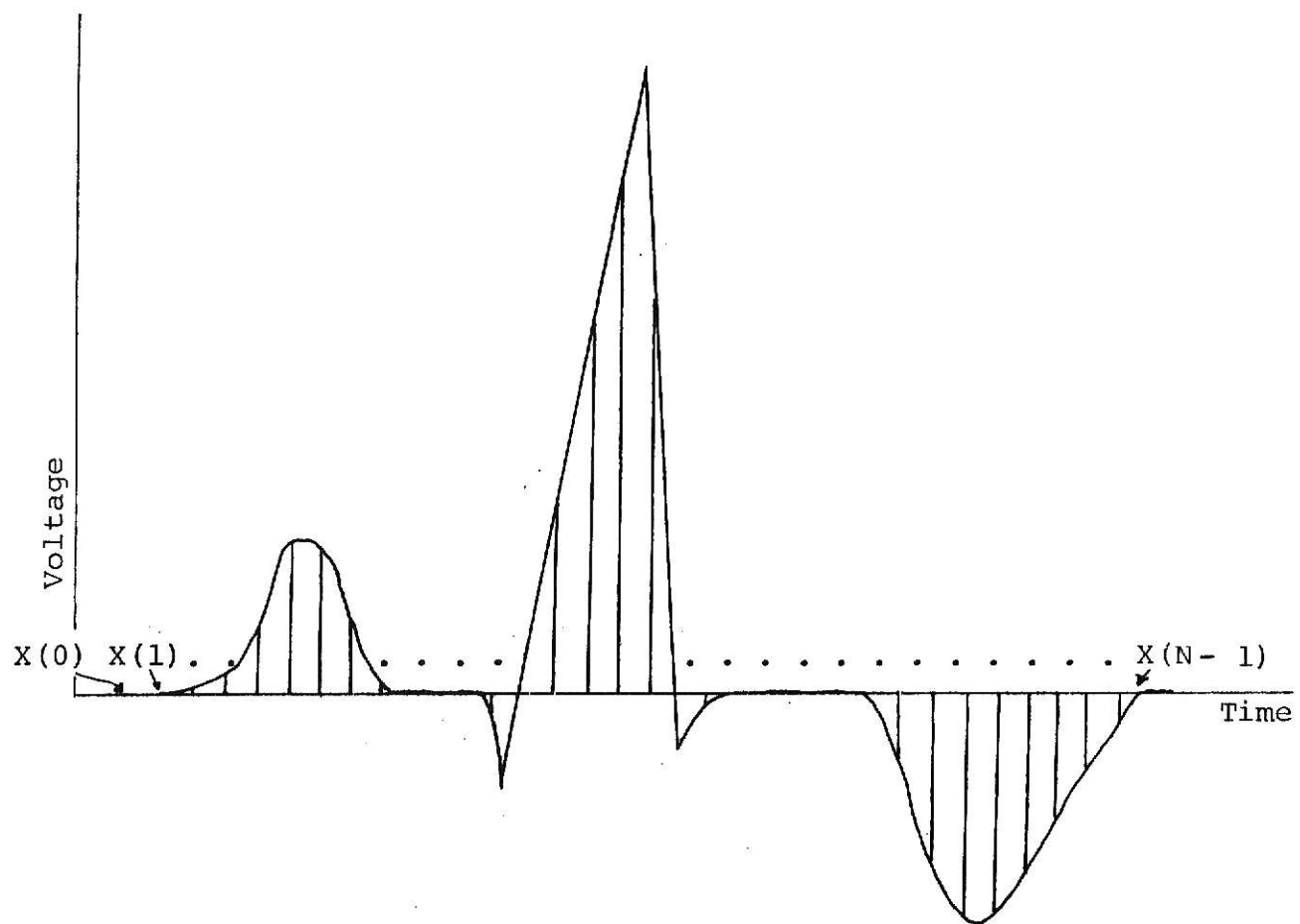
Fig. 5-1. Sampled ECG waveform.

The ECG sampled values $[X(m)]$ can be recovered from the transform coefficients $C_x(k)$ by using the inverse discrete Fourier transform (IDFT) which is defined as

$$X(m) = \sum_{k=0}^{N-1} C_x(k) W^{-km}, \quad m=0,1,2,\ldots,(N-1) \tag{5-2}$$

The physical significance of the DFT is that each $|C_x(k)|^2$ represents the power (i.e., the rate of change of energy) in the kth frequency component of a sampled ECG. The distribution $|C_x(k)|^2$, $k=0,1,\ldots,(N-1)$ is called the DFT power spectrum. For a given ECG the power spectrum has $(\frac{N}{2} + 1)$ independent points given by $|C_x(k)|^2$, $k=0,1,\ldots,(\frac{N}{2} + 1)$. Subsets of this set of $(\frac{N}{2} + 1)$ power spectrum points may be used as ECG signatures. This spectrum can be computed rapidly using an algorithm called the Fast Fourier Transform (FFT) [4].

5.2 Binary Fourier Representation (Bifore)

The Bifore transformation is another orthogonal transformation in which square waves are used in contrast to the exponential functions W^{km} [See 5.1] used in the DFT. These square waves are called Walsh functions. Bifore resembles the Fourier harmonic analysis in geometrical and analytical characteristics. Since the Walsh functions are square waves, they take only two values, namely +1 or -1 as shown in Fig. (5-2) where the first five Walsh functions are pictured. By appropriately sampling Walsh functions, a class of matrices known as Hadamard matrices can be obtained. The elements of these matrices are ±1. Using these matrices it can be shown that [3,37] a transform which is analogous to
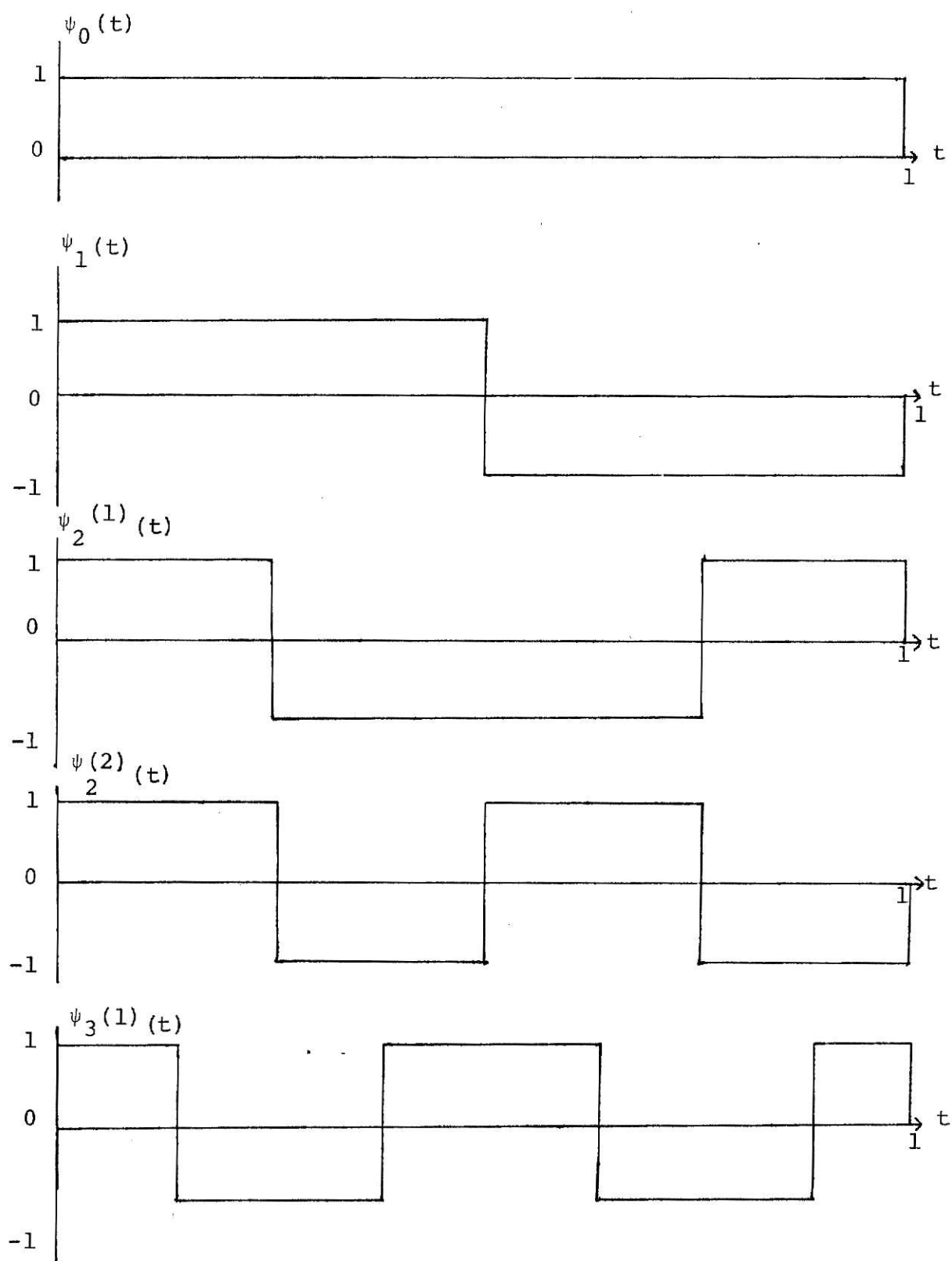
Fig. 5-2. Walsh functions.

DFT can be developed. This transform is known as the Bifore or Walsh-Hadamard transform and is defined as

$$\{B_x(m)\} = \frac{1}{N} [H(n)] \{X(m)\} \tag{5-3}$$

where

$$n = \log_2 N$$

$\{B_x(n)\}$ is a (Nx1) vector whose components $B_x(k)$, k=0,1,..., (N-1) are the BT coefficients
and,

[H(n)] is an NxN Hadamard matrix, and $\{X(m)\}$ represents the sampled values of an ECG in the form of an Nx1 vector.

Again, the ECG can be recovered from the transform coefficient $B_x(k)$, k=0,1,...,(N-1) using the inverse BT (IBT) defined as

$$\{X(m)\} = [H(n)] \{B_x(n)\} \tag{5-4}$$

The BT corresponding to an ECG can be computed rapidly using an algorithm called the Fast Bifore Transform (FBT) which is analogous to the FFT. The FBT for the case N=8 (i.e., 8 sampled values of an ECG) is shown in Fig. (5-3).

5.3 Bifore Transform Power Spectrum

The Bifore transform power spectrum is defined as follows [3,4]:

$$P_O = B_x^2(0)$$

$$P_s = \sum_{k=2^{s-1}}^{2^s-1} B_x^2(k) \quad \begin{matrix} s=1,2,...,n \\ n=\log_2 N \end{matrix} \tag{5-5}$$
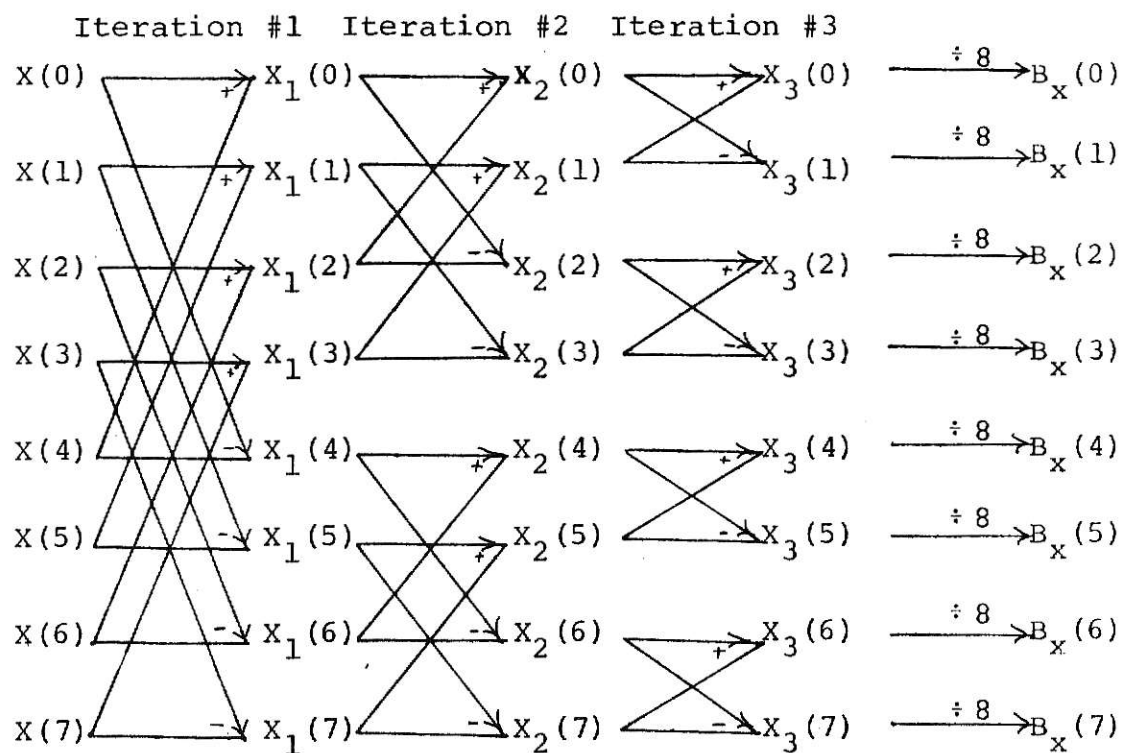
Fig. 5-3. FBT signal flow graph, N=8.

where P_i are the power spectrum points and consist of $\log_2 N+1$ points.

For the example of N=8 the BT spectrum obtained from (5-5) is as follows:

$$P_0 = B_x^2(0)$$

$$P_1 = B_x^2(1)$$

$$P_2 = B_x^2(2) + B_x^2(3)$$

$$P_3 = B_x^2(4) + B_x^2(5) + B_x^2(6) + B_x^2(7)$$

The spectrum defined in (5-5) can be computed rapidly as shown in Fig. (5-4) for the case N=8.

The BT spectrum has two basic properties which are also possessed by the DFT power spectrum. These are as follows:

1. The spectrum points P_i, i=0,1,...,$\log_2 N$ are invariant to shifts of a sampled ECG signal [X(m)].

2. Each P_i represents the distribution of power in an ECG.

On the other hand, while the DFT power spectrum point $|C_x(k)|^2$ yields the distribution of power in an ECG at the frequencies k=0,f_0,2f_0,...., $\frac{N}{2} f_0$, (f_0 being the fundamental frequency*) the BT power spectrum P_i represents the power in a group of frequencies. However, this grouping is not arbitrary. In fact, it can be shown that [2,4] the BT power spectrum is related to the DFT power spectrum as follows:

---

*If T is the duration of an ECG, then the fundamental frequency f_0 is given by $f_0 = \frac{1}{T}$ Hz.
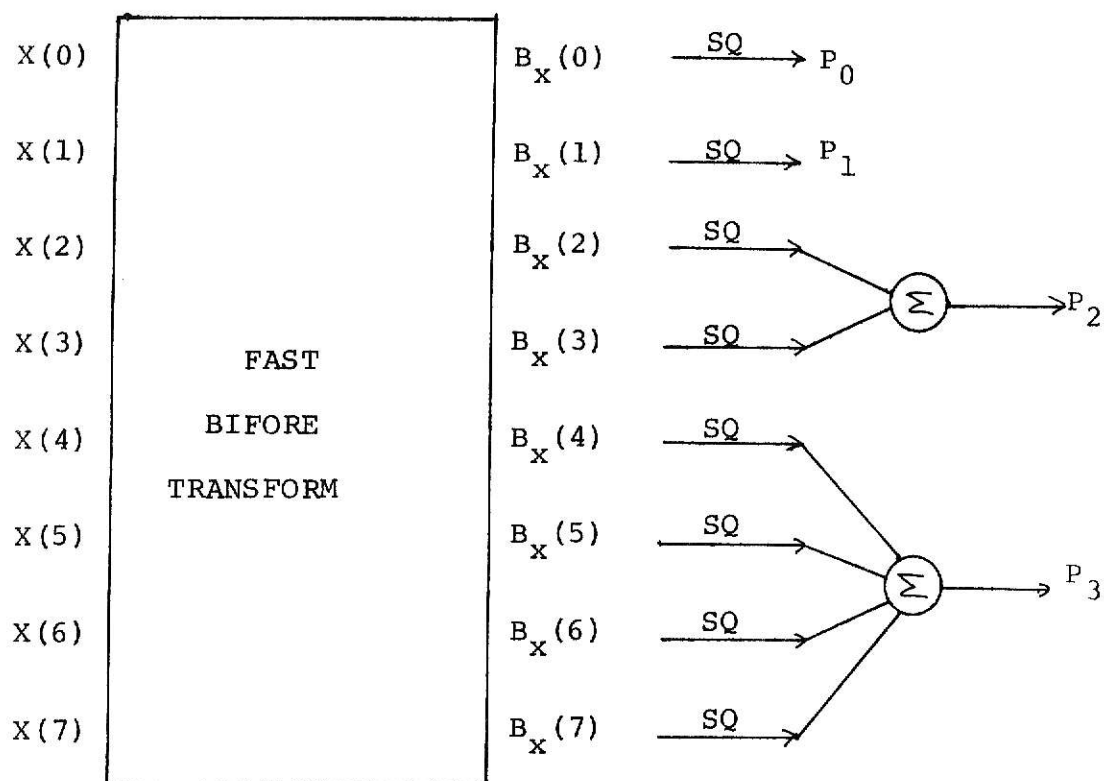
Notation: SQ denotes "square".

Fig. 5-4. Computation of the power spectrum, N=8.

$$P_0 = C_x^2(0)$$

$$P_1 = C_x^2\left(\frac{N}{2}\right)$$

$$P_s = 2 \sum_{k=0}^{2^{s-2}-1} |C_x[2^{n-s}(2k+1)]|^2 \tag{5-6}$$

$$s = 2,3,\ldots,n$$

$$n = \log_2 N$$

From (5-6) it is evident that an inherent property of the BT power spectrum is data compression. That is, while the DFT power spectrum yields a distribution of power which consists of $\left(\frac{N}{2} + 1\right)$ points, the BT power spectrum yields one that consists of $(\log_2 N+1)$ points.

VI

THE CLASSIFICATION PROCESS

After the Bifore power spectrum for the ECGs studied has
been computed using the methods outlined in the previous chapter,
there remains the problem of classification. A classifier is a
device which makes decisions as to what group a given signal
belongs. For example, if the ith and j^{th} signals of the normal
and abnormal ECGs are denoted by $X_{i,n}(t)$ and $X_{j,a}(t)$ respectively,
then the task of the classifier was to assign all the $X_{i,n}(t)$ to
the class of normals and all the $X_{j,a}(t)$ to the class of abnor-
mals. The means by which this task is accomplished will be dis-
cussed in this chapter. In what follows, the terms "class 1"
(C_1) and "class 2" (C_2) will denote the classes of normals and
abnormals respectively.

6.1 Training a classifier

To classify a signal, it first must be identifiable. The
characteristics which serve to identify a given signal are part
of its signature. In this study, the signature used for the pur-
pose of accomplishing this classification is obtained from the
Bifore power spectrum. The signature may be thought of as a
vector and each vector may be thought as going from the origin
to some point in space. Ideally, a given class would be repre-
sented by one point in space. If the signature of a waveform
coincided with the point representing C_1, that signature would
be said to have come from a signal belonging to C_1. As usual,
the real life situation differs from the ideal and we have a

range or group of points which belong to a given class. It then seems logical that some sort of mean, i.e. an average or center of gravity, should be computed for each class. Thus, if $\overline{X}_1$ and $\overline{X}_2$ denote the mean vectors corresponding to C_1 and C_2, then an incoming signature X would be classified as belonging to C_1 or C_2 depending upon whether it is closer to $\overline{X}_1$ or $\overline{X}_2$ respectively. The process by which the mean of a class is determined is called training, while the group of signals used to generate this mean is called the training set. Thus, to train, for example, on the basis of twenty signals, ten known signals belonging to C_1 and ten known signals belonging to C_2 would be used. These twenty signals constitute the training set for the classifier being trained. After the training of the classifier is completed and the means computed, the classifier would be able to make decisions on incoming unknown signatures.

6.2   The Decision Rule Concept

Suppose each signature of class 1 and class 2 is in the form of a 2-dimensional $X = [{}^{X_1}_{X_2}]$. For example, if the signature of class 1 (C_1) and class 2 (C_2) are given by

$$C_1: \quad X_{11} = [{}^5_5], \quad X_{12} = [{}^6_5], \quad X_{13} = [{}^6_6], \quad X_{14} = [{}^6_7], \quad X_{15} = [{}^7_5]$$

$$C_2: \quad X_{21} = [{}^0_3], \quad X_{22} = [{}^{-1}_3], \quad X_{23} = [{}^{-2}_3], \quad X_{24} = [{}^{-3}_3], \quad X_{25} = [{}^{-4}_3]$$

they can be plotted as in Fig. (6-1). A reasonable boundary to separate the two classes could be the perpendicular bisector of the line joining the means (i.e., the averages) of the signatures

of C_1 and C_2. The equation of this line is derived as follows.

Let X be a point on the boundary and $\overline{X}_1$ and $\overline{X}_2$ be the means of class 1 and of class 2 respectively. Then from Fig. (6-1) it follows that:

$$||X-\overline{X}_1|| = ||X-\overline{X}_2|| \qquad (6-1)$$

$$||X-\overline{X}_1||^2 = ||X-\overline{X}_2||^2 \qquad (6-2)$$

where,

$||X||$ denotes the norm. of X. That is,

$$||X||^2 = X'X$$

where,

X' denotes the transpose of X.

Using the above it can be shown that [4]

$$(\overline{X}_1-\overline{X}_2)'X = \frac{1}{2}\{||\overline{X}_1||^2 - ||\overline{X}_2||^2\} \qquad (6-3)$$

For the example of Fig. (6-1) the following results are obtained.

$$\overline{X}_1 = [{}^{6}_{5,6}] \text{ and } \overline{X}_2[{}^{-2}_{3}]$$

Equation (6-3) yields

$$8x_1 + 2.6x_2 = 27.1 \qquad (6-4)$$

Referring to (6-3) the quantity

$$\frac{1}{2}\{||\overline{X}_1||^2 - ||\overline{X}_2||^2\} = 27.1 \qquad (6-5)$$

is referred to as the threshold of the classifier.
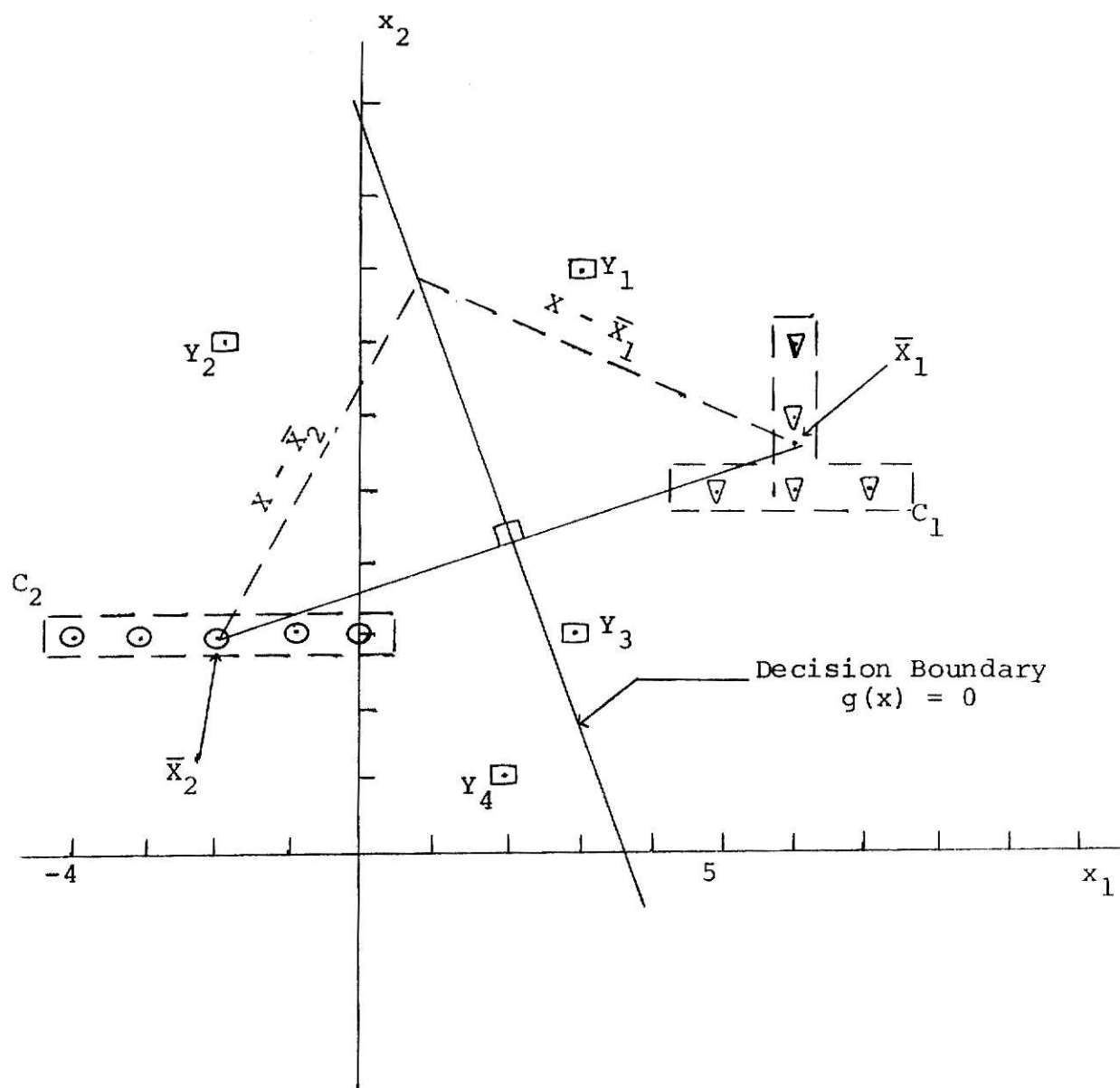
Fig. 6-1. The two dimensional feature space
associated with C_1 and C_2.

Again, the _discriminant function_ (i.e., a function which helps discriminate between C_1 and C_2) is given by

$$g(X) = 8X_1 + 2.6X_2 - 27.1 \qquad (6\text{-}6)$$

g(X)=0 in (6-6) gives the equation to the "decision boundary" which separates C_1 and C_2 as shown in Fig. (6-1). If g(X)<0, then, point X lies to the "right" of the boundary and thus belongs to C_1. If g(X)<0, then X lies to the "left" of the boundary and thus belongs to C_2. If g(X)=0, the point lies on the boundary and the investigator must decide to which class such points should be assigned. A block diagram which implements (6-6) is shown in Fig. (6-2). The unit making the decision on the basis of the above inequalities is called a linear threshold unit and is shown in Fig. (6-2).

6.3 d-Dimensional Measurements [4]

In the previous section, the signature was in the form of a vector which consisted of two components. In general, however, it can consist of d-components. It can then be shown that the discriminant function corresponding to (6-6) is given by

$$g(X) = w_1 x_1 + w_2 x_2 + \ldots + w_d x_d - \theta \, . \qquad (6\text{-}7a)$$

The values w_i, i=1,2,...,d and θ are the "weights" of the classifier. The weight θ is designated as the threshold of the classifier. For this d-dimensional case, the block diagram which implements (6-7) is shown in Fig. (6-3). It follows that (6-7a) can be written as

$$g(\hat{X}) = W'\hat{X} \qquad (6\text{-}7b)$$
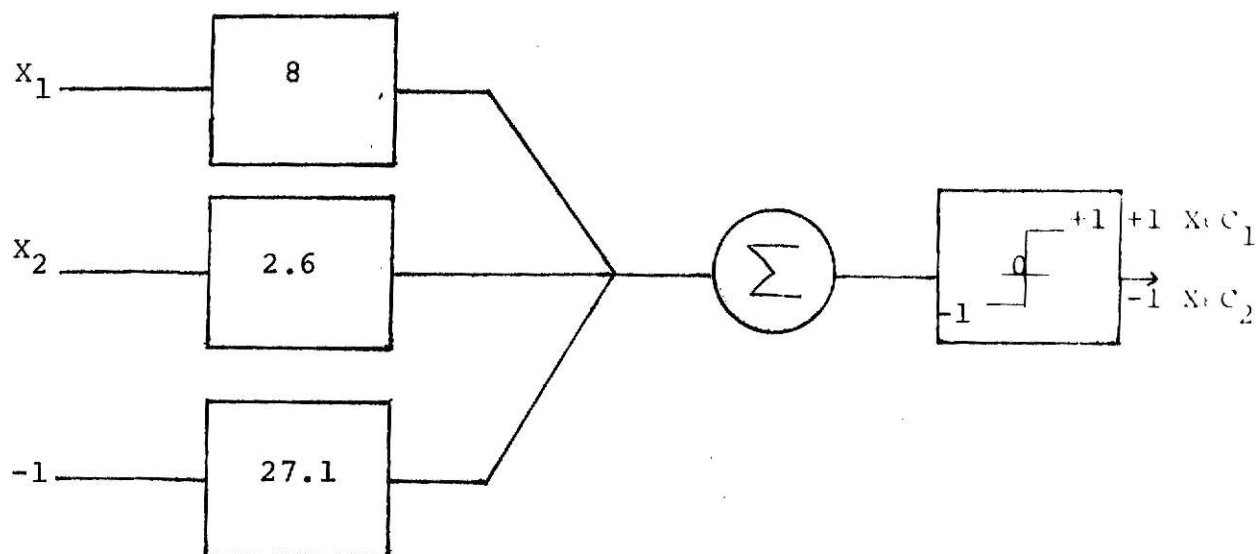
Fig. 6-2. Implementation of classifier for (6-6).
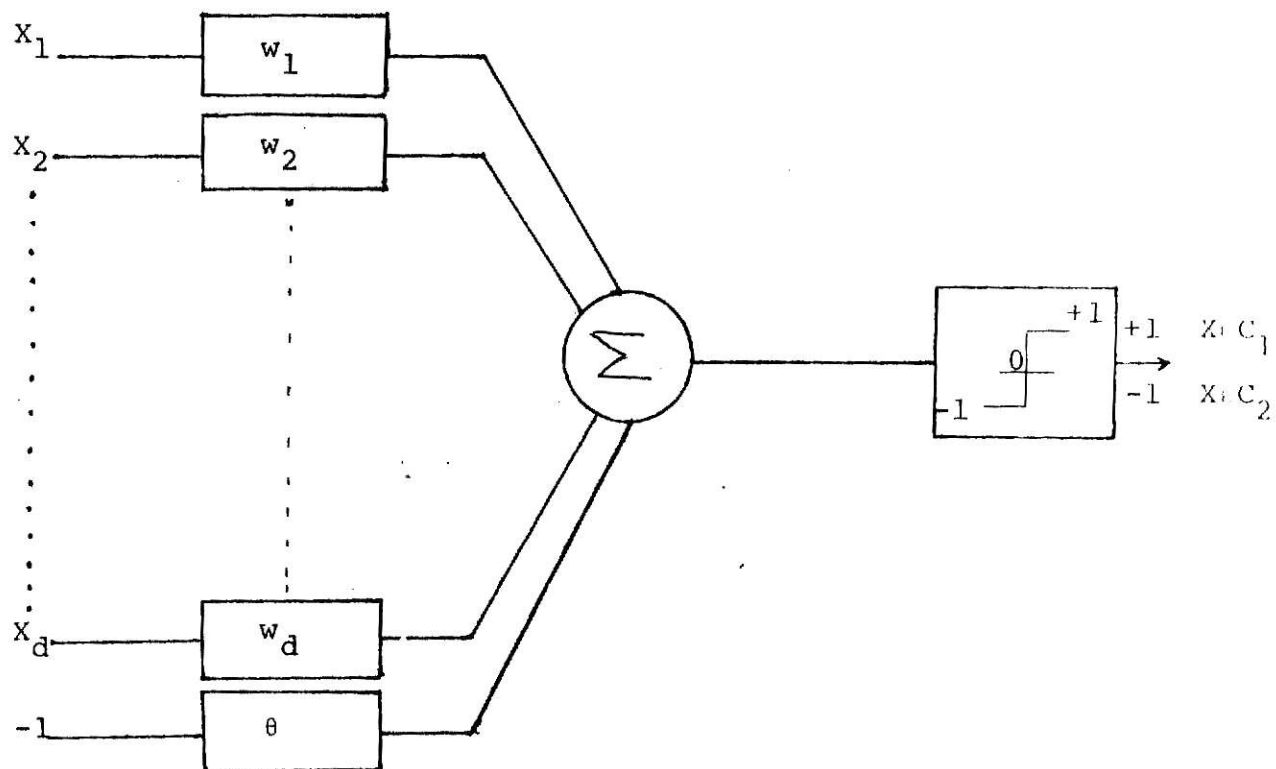
Fig. 6-3. Two class classifier for d dimension pattern vector.

where,

$$W' = (w_1 \quad w_2 \ldots \ldots w_d \quad \theta)$$

and

$$\hat{X}' = (x_1 \quad x_2 \ldots \ldots x_d \quad -1) \quad \text{is called the } \underline{\text{augmented}}$$

vector corresponding to X.

6.5 A Least Squares Classifier [4]

In the above discussion it was tacitly assumed that the signatures pertaining to C_1 and C_2 form tight clusters about their means. In a practical situation, however, this is generally not the case. Thus, to minimize the "spread" of the signatures belonging to C_1 and C_2, an additional transformation is needed. This transformation is illustrated for the case where 2-dimensional signatures are used. Each signature vector in the "signature space" is augmented with a -1 component [see (6-7)] to obtain an "augmented signature space". It can be shown that the desired additional transformation A is obtained by means of the calculation

$$A = [\bar{\hat{X}}_1 - \bar{\hat{X}}_2] [\hat{X}\hat{X}']^{-1} \tag{6-8}$$

where,

$$\bar{\hat{X}}_1 = \frac{1}{N_1} \sum_{j=1}^{N_2} \hat{X}_{2j}$$

$$\bar{\hat{X}}_2 = \frac{1}{N_2} \sum_{j=1}^{N_2} \hat{X}_{2j}$$

$$[\overline{\hat{X}\hat{X}'}] = \sum_{i=1}^{2} \sum_{j=1}^{N_i} \frac{1}{N_i} (\hat{X}_{ij} \quad \hat{X}_{ij}') \quad ,$$

and N_1 and N_2 are the number of training signatures belonging to C_1 and C_2 respectively.

Note that A in (6-8) is a (1x3) vector when X is 2-dimensional. In general, when X is d-dimensional

$$A = [w_1 \quad w_2 \ldots \ldots w_d \quad \theta] \tag{6-9}$$

then A is a [1x(d+1)] row vector of the form (6-9).

In essence, the matrix A maps (using the least square error criterion) the augmented signatures $\hat{X}_{ij}$, $j=1,2,\ldots N_1$ and $\hat{X}_{2j}$, $j=1,2,\ldots,N_2$ in the vicinities of the points $V_1=+1$ and $V_2=-1$ in the decision space as shown in Fig. (6-4)C. The process of training is merely one where the w_i, $i=1,2,\ldots d$ and θ in (6-9) are computed to determine A.

Once A has been obtained, a signature $X' = [x_1 \ x_2 \ x_3 \ldots x_d]$ is identified with C_1 or C_2 as follows:

1. $\hat{X}' = [x_1 x_2 \ldots x_d -1]$ is formed

2. $g(X) = A\hat{X} = w_1 x_1 + w_2 x_2 + \ldots + w_d x_d -1$ is computed

3. If $g(X)<0$, it is decided that $X \epsilon C_1$

   If $g(X)>0$, it is decided that $X \epsilon C_2$

In essence, $g(X)>0$ implies that $Z=A\hat{X}$ which represents the mapping of $\hat{X}$ in the decision space (see Fig. (6-4)C) is closer to $V_1=+1$. Conversely, $g(X)<0$ implies that the mapping of $\hat{X}$ falls closer to $V_2=-1$. The implementation of this classifier is identical to that shown in Fig. (6-3). As mentioned previously, the parameters w_i, $i=1,2,\ldots,d$ and θ are obtained during the training process.
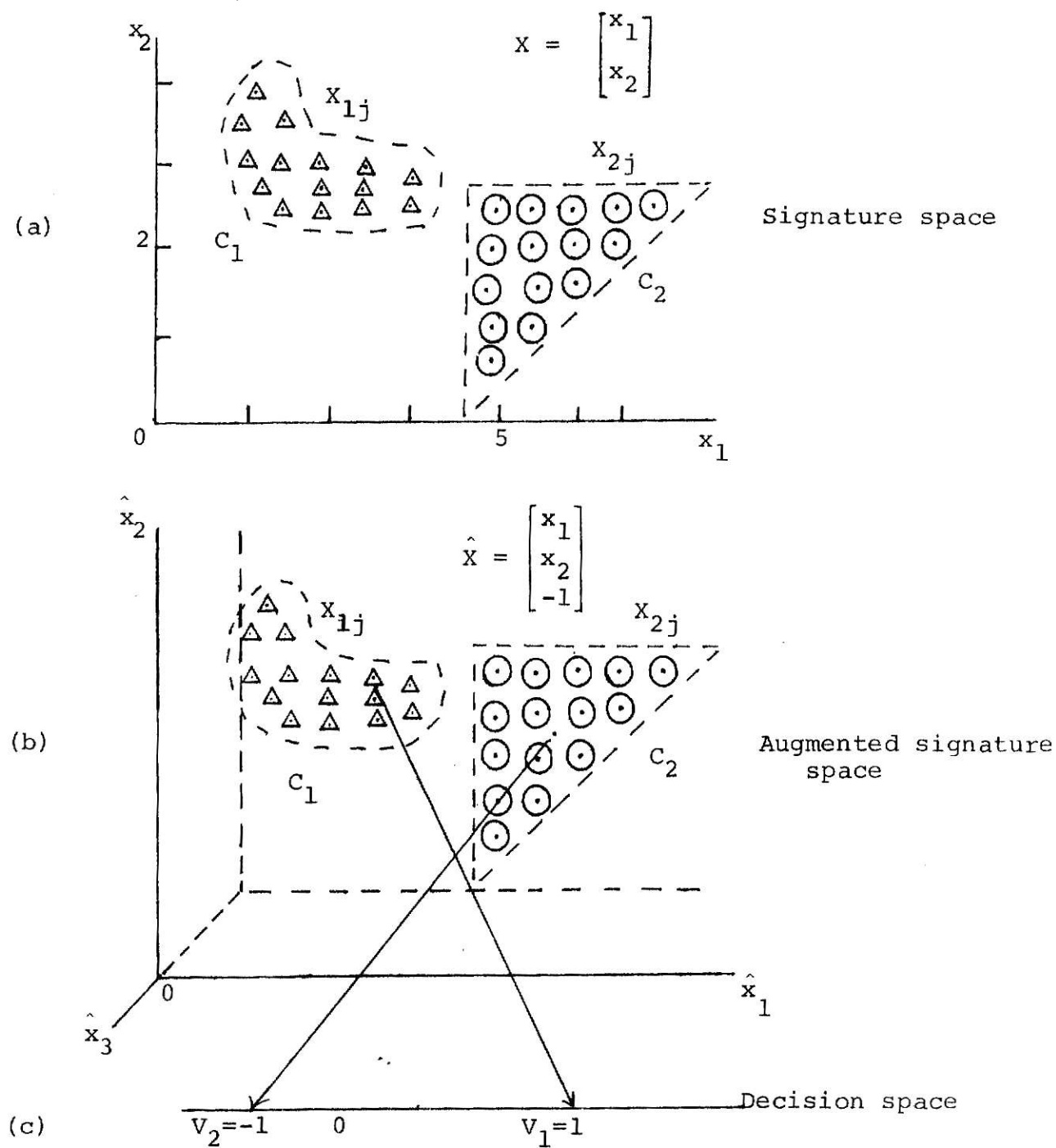
Fig. 6-4. Signature space, augmented signature
space and decision space for a least-
squares minimum distance classifier.

VII

EXPERIMENTAL RESULTS

The purpose of this study was to demonstrate the feasibility of automatically classifying ECG signals using a frequency analysis approach. This study was made using ECG data from the canine. This animal was chosen for study of the ECG because of the similarities between its heart and that of the human. This similarity would then allow the extension of the procedures developed in this study to the human signals. Another reason for the choice of the canine was that it is a readily obtainable laboratory animal and much work has been done with its ECG [18].

7.1 Experimental Procedure

The experimental procedure consisted of anesthesising the canine whose ECG was to be taken to minimize muscle artifact and to make the animal easier to position for the monitoring of its ECG. The X Y Z lead system was chosen since it is a corrected orthogonal lead system which yields a maximum amount of information about the electrical activity of the heart [35]. Two leads were chosen out of these three leads for further study, the X and the Y leads.

The system used to record the data is shown in Fig. (7-1). It consisted of an Electronics for Medicine model DR-8 recording system. This unit contained the necessary ECG amplifiers, a cathode ray display, balancing amplifiers for recording and a photographic paper recorder. A Hewlett Packard model 3960A tape recorder was used to record the data. This recorder was
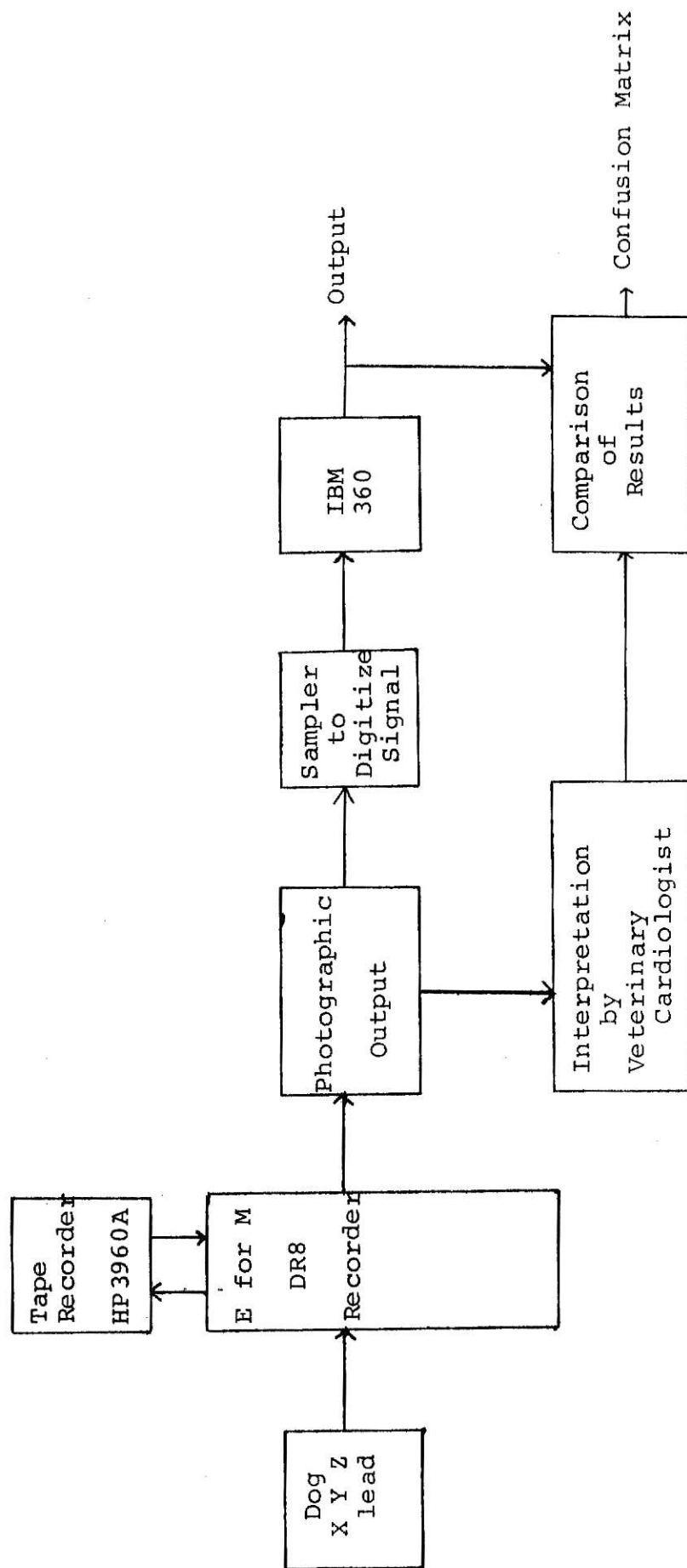
Fig. 7-1. System used for classification.

of the four channel, FM type. It was used at 7 1/2 ips (inches
per second) to record and 3 3/4 ips to play back. The recorded
signals were then played back through the Electronics for Medicine
system and recorded on light sensitive photographic paper. The
frequency response of this system was more than adequate for
minimizing distortion of the ECG signal. [17,23]

It was desired to record both normal and abnormal ECGs
from the same three experimental animals. The determination of
normal and abnormal was made by the veterinary cardiologist at
Kansas State University's Dykstra Veterinary Hospital. The
normal ECG for the animal under study was first recorded. By
mechanical and chemical stimuli, this normal ECG was altered.
These altered or abnormal ECGs were then recorded. By recording
the data in the above manner, it was possible to study the charac-
teristics of normal vs. abnormal ECGs in two ways. First, ECGs
from the three dogs could be mixed and the characteristics of
normal vs. abnormal ECGs in this mixed population could be studied.
Secondly, the relationship between normal and abnormal ECGs in
a given subject could be studied.

The QRS complex of the ECG was chosen as the characteristic
of the ECG to be used to classify the signals. This segment was
chosen because it is one of the easier segments of the ECG for
an automated system to recognize due to its large positive and
negative slopes [40,42]. It was also chosen since many common
abnormalities may be recognizable due to their QRS configurations
[18, 22]. In using this one segment, problems of recognizing the
other segments of the ECG and of the varying time durations be-

tween segments could be avoided.

Since the digital computer was to be used in the classification of the data, it was necessary to digitize the data. Using the data obtained from the X and Y leads this was done in the following manner. The ECG which had been recorded on photographic paper was photographed on 35 mm Kodak Tri X negative film using a Nikon F camera with a 50 mm f 2.0 Nikkor lens and Nikkor K1 and K2 extension tubes. The resulting negative was processed and projected onto the screen of a microfilm reader. On the screen of this reader was a grid designed to sample the QRS complex 32 times. The values of the amplitude of each of these samples were then entered on standard IBM data cards for processing by the IBM 360 computer.

7.2 Frequency Analysis of ECG Data

Figure (7-2) shows the two channels of information used in this study. The QRS portion of the ECG was sampled 32 times and each sample consisted of two components $X_1(i)$ and $X_2(i)$ where $i=1,2,\ldots,32$. $X_1(i)$ is the value of the ith sample from the X channel while $X_2(i)$ is the value of the ith sample from the Y channel. The two channels were sampled simultaneously thus, $X_1(i)$ and $X_2(i)$ were determined at the same point in time. The result of this sampling of the X and Y leads of the ECG is a 2 x 32 matrix of the form

$$\begin{bmatrix} X_1(i) \\ X_2(i) \end{bmatrix} = \begin{bmatrix} X_1(0) & X_1(1) & X_1(2)\ldots X_1(31) \\ X_2(0) & X_2(1) & X_2(2)\ldots X_2(31) \end{bmatrix} . \qquad (7-1)$$
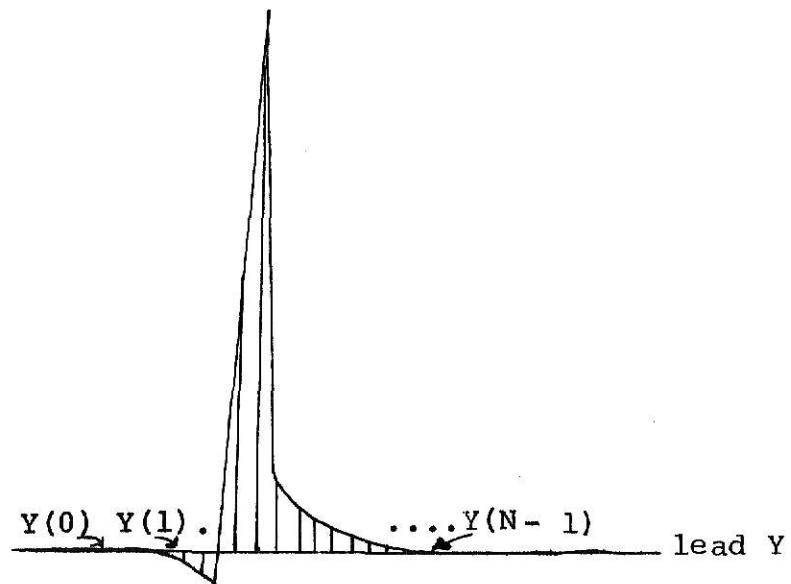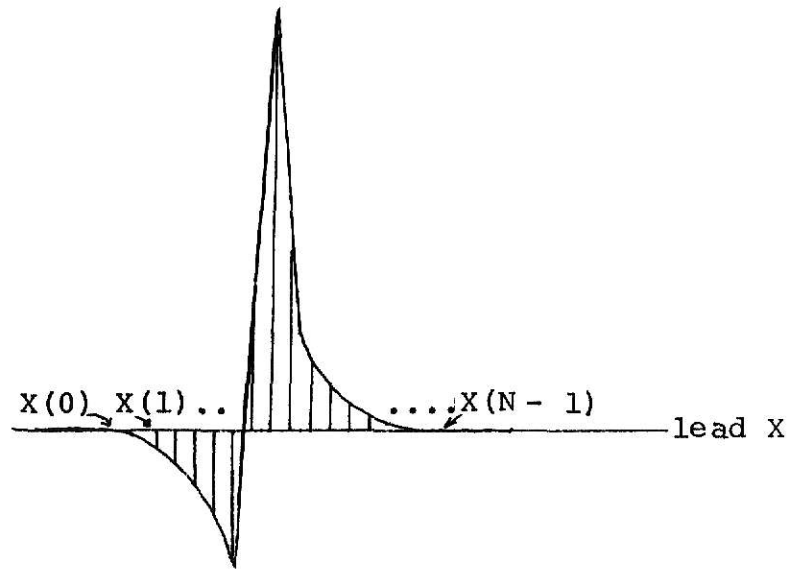
Fig. 7-2. Sampled QRS segments obtained
          from leads X and Y.

The two-dimensional form of the Bifore transform discussed in Chapter 5 was used. The application of the two dimensional BT is exactly equivalent to applying the one dimensional BT to the sum of channels X and Y and then applying it to the difference of channels X and Y. Since each of these applications will involve 32 data points each will yield a 6 component power spectrum. The total result for the two dimensional BT power spectrum will be 12 components as shown by Fig. (7-3).

7.3 Selection of BT Spectrum Points as Signatures

The next step towards the goal of automating the analysis of the ECG was to choose the characteristics from the power spectrum obtained and shown in Table (7-1) to be used in the classification process. Upon examination of the data of Table (7-1), it was decided that much of the variation between normal and abnormal ECGs is contained in components 5,6,11, and 12 of the Bifore power spectrum. It was further decided that these components would be used in the classification process. These components are the ones that combine the high frequency DFT power spectrum points, as discussed in Chapter 5. Figures (7-4) and (7-5) show the two dimensional plots of component 5 vs. 6 and component 11 vs. 12. The separation of normal from abnormal in both plots suggested that two or more components would characterize the signal for classification purposes. The least squares classifier discussed in Chapter 6 (section 5) was used to classify normal and abnormal ECGs. The classifier was trained with a known set of ten signals belonging to the normal class and ten

P_0 P_1 P_2 P_3 P_4 P_5 From X + Y

P_6 P_7 P_8 P_9 P_{10} P_{11} From X - Y

Fig. 7-3.   Power spectrum points
            for 2 channels of 32
            samples.

Figure 7-4. Component 6 vs. Component 5
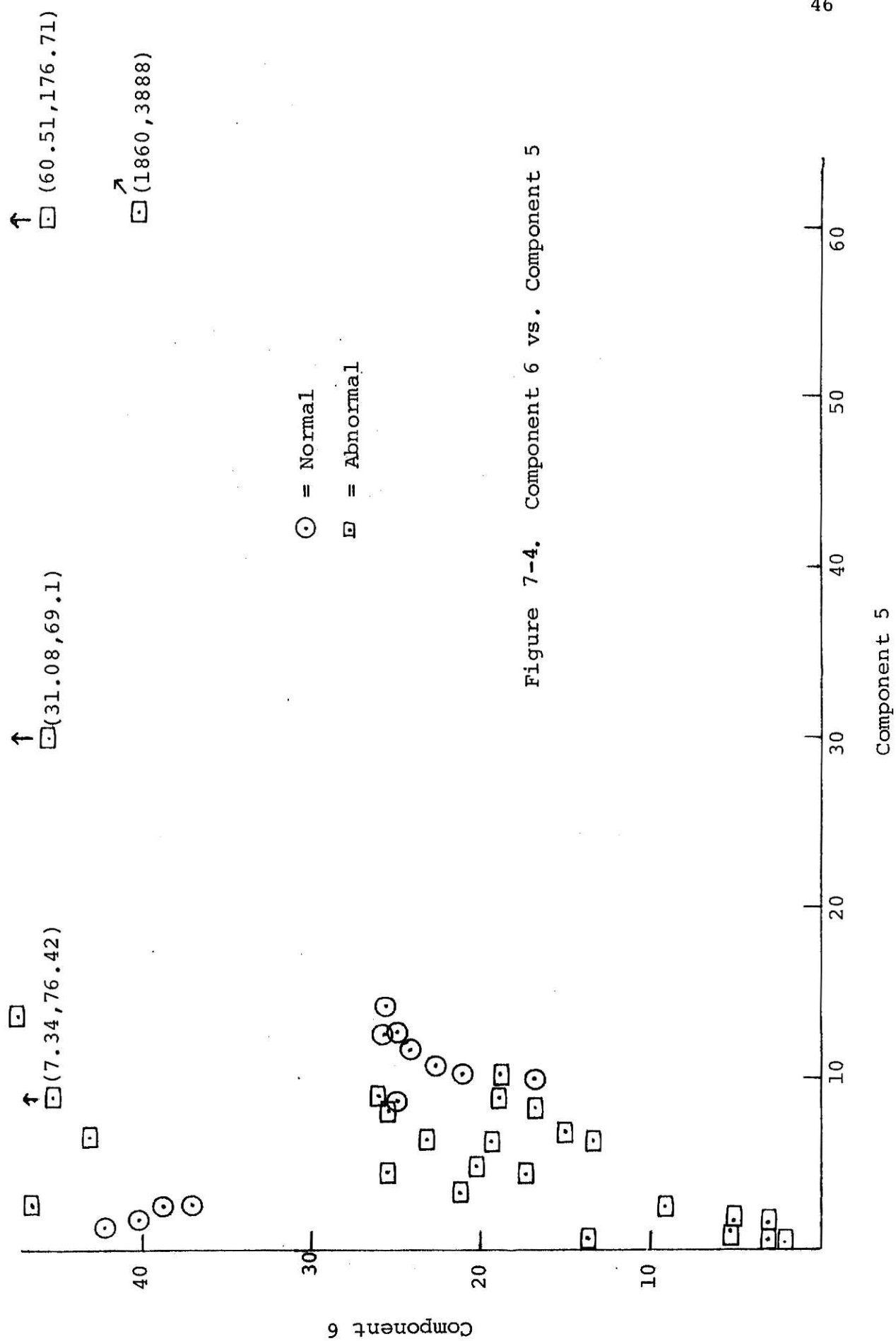
Fig. 7-5. Component 11 vs. Component 12

ILLEGIBLE DOCUMENT

THE FOLLOWING
DOCUMENT(S) IS OF
POOR LEGIBILITY IN
THE ORIGINAL

THIS IS THE BEST
COPY AVAILABLE

P-474

Table 7-1 Biforo spectrum points

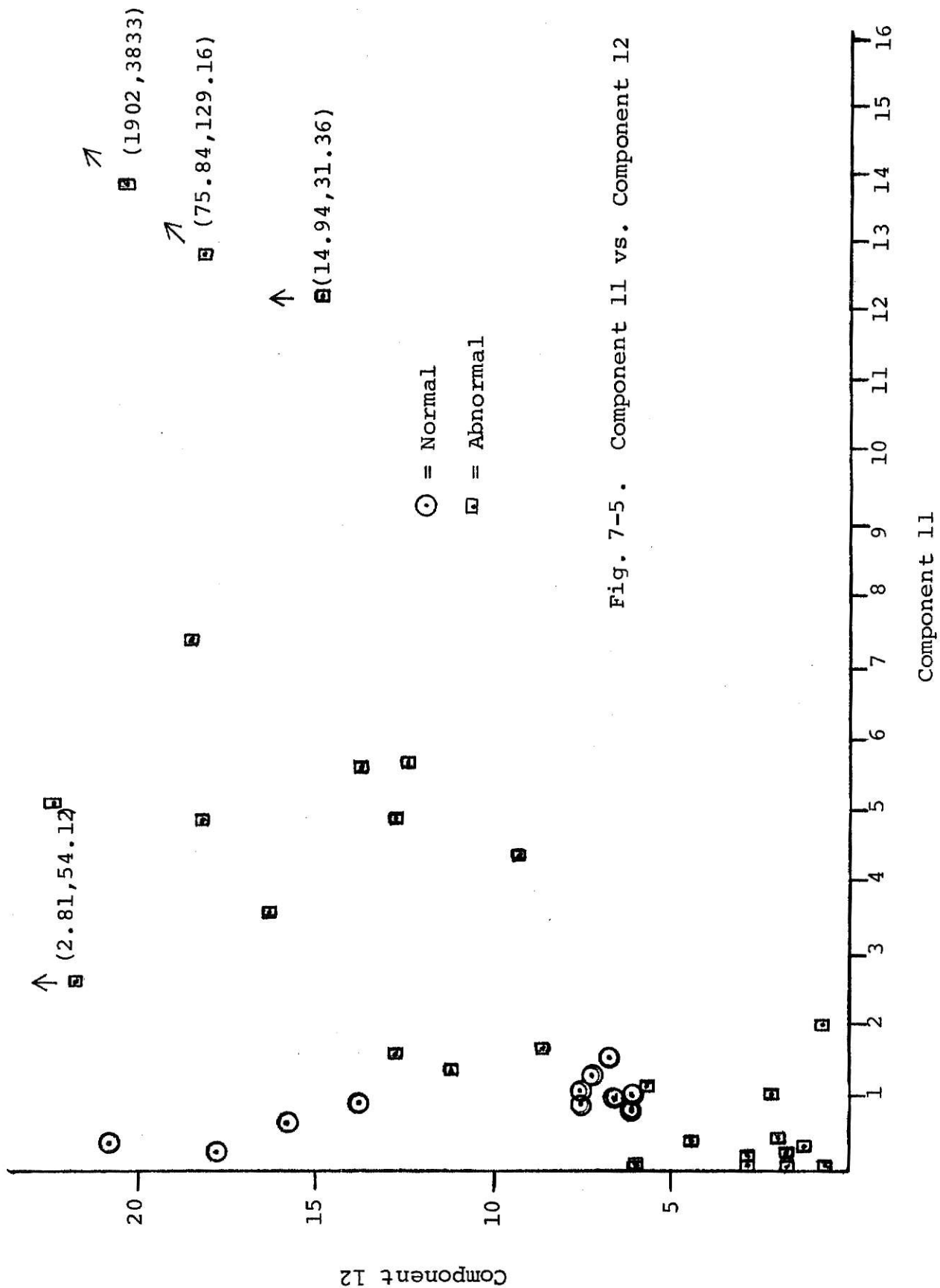| POG	CLASS	1	2	3	4	5	6	7	8	9	10	11	12
(1,8)	N	21.77	0.00	.01	.03	2.32	37.00	19.5	0.00	0.00	0.10	0.34	20.30
(1,9)	N	27.24	0.00	0.00	0.06	1.94	41.07	14.87	0.00	.02	.11	.63	15.03
(1,12)	N	24.64	0.00	0.00	.03	2.62	38.60	14.69	0.00	0.00	.01	.29	17.39
(1,11)	N	23.45	0.00	.01	.08	1.53	42.67	18.85	0.00	0.00	0.11	.93	13.90
(3,1)	N	10.19	0.00	0.02	0.23	14.21	25.93	2.36	0.00	0.01	0.27	1.01	6.10
(3,2)	N	6.19	.03	.04	.46	10.03	16.82	2.00	0.02	0.05	0.61	1.11	11.16
(3,5)	N	10.78	0.00	0.00	0.68	13.14	25.04	2.71	0.00	0.00	0.39	1.16	7.44
(3,6)	N	10.05	0.00	0.01	.19	10.70	23.19	2.11	0.00	0.00	0.14	1.34	7.11
(3,7)	N	9.50	0.00	0.00	0.41	12.55	25.62	1.91	0.00	0.00	0.21	0.96	7.38
(3,8)	N	8.39	0.00	0.00	0.36	11.92	24.09	1.76	0.00	0.00	0.45	0.97	6.14
(3,9)	N	8.93	0.00	0.01	0.16	9.34	25.04	3.36	0.00	0.00	0.45	1.51	6.77
(3,10)	N	7.00	0.00	0.01	0.63	10.14	21.02	1.61	0.01	0.01	0.24	1.06	6.38
(1,1)	N	1.68	0.00	0.00	0.40	1.09	4.87	8.22	0.00	.02	.33	7.44	18.12
(1,2)	A	11.38	0.00	.01	.49	6.12	19.54	.65	0.00	0.01	0.07	1.12	5.78
(1,3)	A	19.84	1.84	4.28	10.36	31.08	69.10	.02	1.97	3.83	7.73	14.94	31.30
(1,4)	A	34.20	9.16	17.15	39.02	60.51	176.77	3.64	8.44	17.52	32.74	15.84	129.10
(1,5)	A	18.87	0.00	0.00	.03	4.39	25.66	0.18	0.00	0.01	0.25	0.45	4.39
(1,6)	A	9.88	0.00	0.01	0.28	9.59	25.85	2.77	0.00	0.01	0.27	1.66	8.61
(1,7)	A	9.03	0.00	0.01	0.14	9.36	25.04	4.29	0.00	0.00	0.11	1.46	11.16
(1,10)	A	211.2	.13	.40	1.97	6.86	43.29	4.66	.01	.01	.02	.31	1.94
(1,14)	A	23.57	.04	.18	.84	2.20	8.74	3.27	.01	.04	.15	.39	1.47
(1,13)	A	46.45	0.00	0.00	09	.37	13.49	4.14	0.00	.01	.06	.04	2.77
(2,1)	A	8.95	0.00	.01	.37	9.59	18.40	5.25	.01	.07	.06	4.47	9.28
(2,2)	A	15.66	0.00	.01	.01	5.32	20.18	13.29	0.00	0.00	0.18	3.67	16.41
(2,3)	A	16.73	0.00	0.00	.39	6.20	23.17	10.36	0.00	0.00	.08	1.66	12.87
(2,4)	A	7.89	0.00	.05	.13	8.58	16.58	7.60	0.00	.03	.52	5.60	13.71
(2,5)	A	11.05	.01	.01	.16	4.53	17.45	10.13	0.00	.02	.59	4.82	18.99
(2,6)	A	8.45	0.00	.01	.43	10.07	18.78	7.6	0.00	.02	.33	5.82	12.80
(2,7)	A	13.92	0.00	0.00	0.14	3.50	21.04	12.25	0.00	0.01	0.39	5.08	22.41
(2,8)	A	54.05	.15	.45	1.82	7.34	76.42	8.18	0.00	.02	.11	1.07	1.76
(2,9)	A	6.30	0.00	0.00	.04	.54	2.93	1.55	0.00	.01	.14	.17	2.98
(2,10)	A	8.79	0.00	0.00	.01	1.30	2.61	1.93	0.00	0.00	.08	.04	1.47
(2,11)	A	15.25	0.00	.02	.10	1.23	4.79	1.68	0.00	0.00	.03	2.08	.31
(2,12)	A	474.08	239.72	474.13	935.85	1860.12	3888.87	289.58	236.44	467.99	939.06	1902.71	3845.57
(2,13)	A	75.77	.06	.28	1.32	11.45	60.92	10.88	0.00	0.00	.01	.18	5.34
(2,14)	A	4.94	0.00	.01	.17	7.12	14.82	8.23	0.00	.05	.52	5.75	12.13
(3,11)	A	17.31	.06	.15	.45	6.30	13.33	.16	0.00	.02	.07	.27	1.22
(3,12)	A	2.9	0.00	.02	.03	.22	1.26	.14	0.00	0.00	.02	.02	.41
(3,18)	A	23.19	.02	.04	.23	2.53	59.49	46.97	0.00	0.00	.26	2.81	54.12

N: NORMAL
A: ABNORMAL

signals belonging to the abnormal class. It was then tested as to how well it classified this training set. The resultant was the so-called confusion matrix in which the diagonal terms show correct decisions and the off diagonal terms show the incorrect decisions. The general form of this matrix is shown in Fig. (7-6).

7.4 Significance of the Confusion Matrix

Tables (7-2), (7-3) and (7-4) show the results of the different training sets used in the training of the two-class classifier. Normals were obtained only from dogs #1 and #3. Table (7-2a,b) and (7-3c,f) show the correct classification of all normals and abnormals within a given dog. This suggested the possibility of applying this technique to a monitoring situation. The two components used as a result of the two channels of information X and Y were more successful in this classification process than the two components obtained with the one dimensional transform using the X lead only. This result can be seen by comparing Tables (7-2a,b,c) and (7-3a,b,c).

The three dog's ECGs were then mixed. The problem at this point involved finding the best combination of the Bifore power spectrum points to separate the normals from abnormals for this mixed case. Tables (7-2c,e,f) and (7-3c) show the results of these attempts. Using the X lead only as in Table (7-3c) results in eight abnormals being classed as normal. When the two channels of ECG data are used, the results in Table (7-2c,d,e,f) are obtained. Table (7-2c) shows six errors of the abnormal type being classed normal type using components 11,12. In Table (7-2d),

$$
\begin{bmatrix}
N(1,1) & N(1,2) \\
N(2,1) & N(2,2)
\end{bmatrix}
$$

$N(i,j)$ indicates that a signal from class "j" has been classed as belonging to class "i".

Fig. 7-6.   The confusion matrix.

51

Table 7-2 matrices:

(a) $\begin{bmatrix} 10 & 0 \\ 0 & 10 \end{bmatrix}$ Dog #1 (11,12)

(b) $\begin{bmatrix} 10 & 0 \\ 0 & 10 \end{bmatrix}$ Dog #3 (11,12)

(c) $\begin{bmatrix} 10 & 6 \\ 0 & 4 \end{bmatrix}$ Dogs #1,2,3 (11,12)

(d) $\begin{bmatrix} 6 & 2 \\ 4 & 8 \end{bmatrix}$ Dogs #1,2,3 (5,6)

(e) $\begin{bmatrix} 9 & 3 \\ 1 & 7 \end{bmatrix}$ Dogs #1,2,3 (6,11,12)

(f) $\begin{bmatrix} 10 & 3 \\ 0 & 7 \end{bmatrix}$ Dogs #1,2,3 (5,6,11,12)

Table 7-2   Two-channel results for the training set in form of confusion matrix.

Table 7-3 matrices:

(a) $\begin{bmatrix} 10 & 2 \\ 0 & 8 \end{bmatrix}$ Dog #1 X lead only (5,6)

(b) $\begin{bmatrix} 10 & 3 \\ 0 & 7 \end{bmatrix}$ Dog #3 X lead only (5,6)

(c) $\begin{bmatrix} 10 & 8 \\ 0 & 2 \end{bmatrix}$ Dogs #1,2,3 X lead only (5,6)

Table 7-3   Results of classification of one-channel data.

Table 7-4 matrices:

(a) $\begin{bmatrix} 10 & 2 \\ 0 & 8 \end{bmatrix}$ Normal Dog #3 Abnormal Dog #2 (5,6,11,12)

(b) $\begin{bmatrix} 10 & 0 \\ 0 & 10 \end{bmatrix}$ Normal Dog #3 Abnormal Dog #1 (5,6,11,12)

(c) $\begin{bmatrix} 10 & 0 \\ 0 & 10 \end{bmatrix}$ Normal Dog #3 Abnormal Dog #3 (5,6,11,12)

(d) $\begin{bmatrix} 10 & 0 \\ 0 & 10 \end{bmatrix}$ Normal Dog #1 Abnormal Dog #3 (5,6,11,12)

(e) $\begin{bmatrix} 10 & 0 \\ 0 & 10 \end{bmatrix}$ Normal Dog #1 Abnormal Dog #2 (5,6,11,12)

(f) $\begin{bmatrix} 10 & 0 \\ 0 & 10 \end{bmatrix}$ Normal Dog #1 Abnormal Dog #1 (5,6,11,12)

Table 7-4   Results of classification of mixed groupings of signals obtained from two channels.

six errors were again made but only four were abnormals classed as normal and two were normals classed abnormal. These results were obtained using components 5 and 6 for the classification process. In the next step, three components were used and the results are shown in Table (7-2e). Only four errors were made, three of the abnormal classed normal type and one of the normal classed abnormal type. To further reduce the number of errors being made, the four power spectrum components 5,6,11, and 12 were used and the results are shown in Table (7-2f). The number of errors was reduced to three of the abnormal classed normal type. The above results were all obtained by using ten normal and ten abnormal ECGs to train the classifier and then using the trained classifier to classify these same training signals. The actual classification is made by taking the dot product of the pattern vector in question with the decision numbers obtained in this training process. .Chapter 6 discusses this process.

The errors in classification seemed to be caused by the existence of two modes of normal, one for dog #1 and one for dog #3. The bimodal effect was eliminated by using the normals from one dog at a time with one set of abnormals at a time. The results are shown in Table (7-4). The normals from one dog separate well from the abnormals of each of the other dogs and of the given dog as shown by the combinations studied. These confusion matrices again came from the training set as previously described.

Once the decision numbers are obtained, it is possible to take signals from outside of the training set, obtain their

pattern vector, form their Bifore power spectrum and then use the decision numbers from the training set to classify these signals. Table (7-5) shows the results obtained using the decision numbers from the training process to classify the complete set of signals. In Table (7-5a) the three components used were 6, 11, and 12. Eleven errors were made out of fifty-four signals being classified. In Table (7-5b) the four components 5, 6, 11 and 12 were used and the results were eight errors of the abnormal classed normal type for an efficiency of better than eighty-five per cent.

$$\begin{bmatrix} 25 & 9 \\ 2 & 18 \end{bmatrix}$$

Dogs #1,2,3
(6,11,12)

(a)

$$\begin{bmatrix} 27 & 8 \\ 0 & 19 \end{bmatrix}$$

Dogs #1,2,3
(5,6,11,12)

(b)

Table 7-5   Results of using decision numbers in classifying ECG data from all three dogs.

VIII

CONCLUSIONS

The result of this study suggest three plausible uses for
the application of Bifore frequency analysis to ECG data. First
of all, in patient monitoring one normal or acceptable ECG would
be obtained for the individual being monitored. This "normal"
might actually be an abnormal signal but would be an acceptable
steady state signal for the individual at that time. This "normal"
would be compared to a large class of previously collected ab-
normal signals continuously and any change from the "normal"
would be detected. This application is strongly supported by
the success of the classifier in separating normal and abnormal
ECGs in a given dog. A second, related, application would be
to use the techniques developed in serial electrocardiography.
Serial electrocardiography involves the taking of the individual's
ECG while he is in the normal state for comparison at a future
time. It would become part of his medical history. Any changes
would signify the onset of heart malfunctionings. Mass screening
is the third application. In this case large amounts of normal
and abnormal ECGs would be collected for use in training a classi-
fier which would be used in any situations where mass screening
would be necessary.

In any of the above applications an alternate approach to
the least square error classifier should be investigated. This
alternate approach would use the cross correlation between a
known and an unknown signal's Bifore power spectrum as a basis

for classification. The unknown signal would be classed as a member of the group to which it had the highest correlation. This approach should also be compared to the straightforward cross correlation of the time domain samples to determine whether the Bifore power spectrum is more "sensitive" to changes in the ECG.

The implementation of the procedures described above would be as shown in Fig. (8-1). The screening system would consist of one box with the decision numbers wired into it. In the patient monitoring or the serial application this box would consist of adjustable decision parameters. These parameters would be obtained by running a few traces of the individual's ECG through the system in Fig. (8-2). Thus, the monitoring facility would need only one large system to determine the parameters to be used in the classifier. The classifier itself would be small and relatively inexpensive enabling a large number to be economically used in the examining facility. These same monitoring devices could be used for mass screening or the simpler "hard wired" units could be used.

The classifier used in this study was of the least squares linear type. Possibly correlation or nearest neighborhood type classifiers could be used instead. These alternate approaches to the classifier would still use the data from the frequency analysis as features or characteristics. In future work, it is suggested that larger quantities of data be collected to further support the results of this preliminary study. An automated system to take the data from the tape recorder to the computer would be of great value in amassing this data. It possibly would
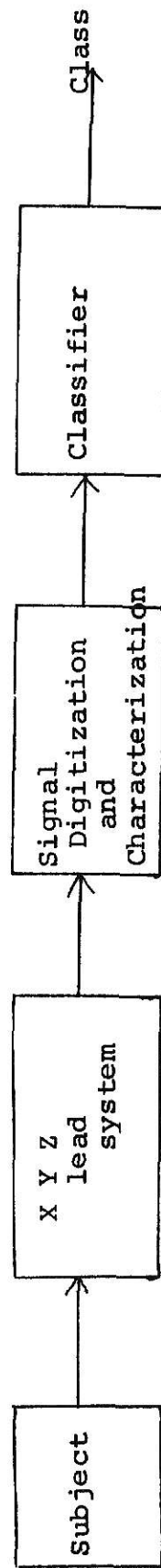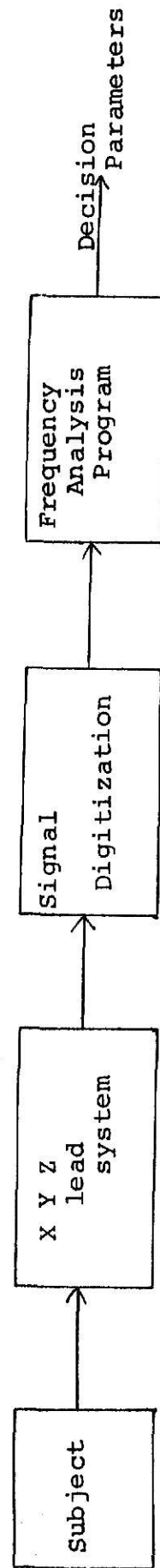
Fig. 8-1. ECG classification system.

Fig. 8-2. System for obtaining the decision parameters.

give better results with the elimination of the human sampling errors. This device then would be incorporated into the final data processing system. One of the most serious problems encountered was due to the multi-modal character of both the normal and the abnormal signals. A further study should determine if there are a finite number of these modes and what they represent. The classifier would then be multi-modal in nature and perhaps with a correlation or nearest neighbor classifier the different abnormalities could be classified as subclasses of the abnormal. The same could be done for the different normal modes.

The classifier is dependent on the choosing of the most significant characteristics as a basis for classification. In future studies, the intermediate invariants might be studied in an attempt to choose more significant characteristics than those presented in this study. Perhaps these results could be combined with the present characteristics for even better classification results.

Preprocessing would also make the classification process more efficient by filtering out some more obvious abnormal recordings. The limits of the normal QRS interval could be set and those signals outside of these set normal limits would be declared abnormal in this first step. Any additional information is of great value to the classifier. For example, in the case of the monitoring device, often times the physician expects certain abnormalities to occur after a certain type of illness. In the training of the classifier, this would enable it to eliminate some modes from its training set making the classifier

more efficient.

In summary, this study has demonstrated the feasibility of using frequency domain characteristics to analyze electrocardiographic data. Further studies should include the analysis of more data, searching for other significant features of the QRS complex, preprocessing and using any other available information to improve the efficiency of the classification process. The goal is to develop a system that will efficiently, economically, and conveniently analyze electrocardiographic data.

IX

BIBLIOGRAPHY

1. Ahmed, N., Rao, K.R. and Schultz, R.B. The Generalized Transform, Applications of Walsh Functions, Proceedings: 60-67. 1971.

2. Ahmed, N. and Bates, R.M. A Power Spectrum and Related Physical Interpretation for the Multi-Dimensional Bifore Transform. Applications of Walsh Functions. Proceedings: 45-50. 1971.

3. Ahmed, N., Rao, K.R., and Abdussattar, A.L. Bifore or Hadamard Transform. IEEE Transactions on Audio and Electro-acoustics AU 19: 225-234. 1971.

4. Ahmed, N. Personnal communication. Kansas State University. Manhattan, Kansas.

5. Alexander, D. and Wortzman, D. Computer Diagnosis of Electrocardiograms. I Equipment. Computers and Biomedical Research 1: 348-365. 1968.

6. Barker, J.E. Investigation of Several Normal and Abnormal Electrocardiographic Waveforms in the Frequency Domain. Master's Thesis Iowa State University of Science and Technology. Ames, Iowa. 1966.

7. Berson, A.S. and Pipberger, H.V. Electrocardiographic Distortions Caused by Inadequate High Frequency Response of Direct-Writing Electrocardiographs. American Heart Journal 74: 208-218. 1967.

8. Berson, A.S. and Pipberger, H.V. The Low-Frequency Response of Electrocardiographs, a Frequent Source of Recording Errors. American Heart Journal 71: 779-789. 1966.

9. Bonner, R.E. and Schwetman, H.D. Computer Diagnosis of Electrocardiograms. II. A Computer Program for EKG Measurements. Computers and Biomedical Research 1: 366-386. 1968.

10. Bonner, R.E. and Schwetman, H.D. Computer Diagnosis of Electrocardiograms. III. A Computer Program for Arrhythmia Diagnosis. Computers and Biomedical Reserach 1: 387-407. 1968.

11. Caceres, C.A. et al Computer Extraction of Electrocardio-graphic Parameters. Circulation XXV:356-361. 1962.

12. Caceres, C.A. How Can the Waveforms of a Clinical Electro-cardiogram be Measured Automatically by a Computer? IRE Transactions on Bio-Medical Electronics 9: 21-22. 1962.

13. Caceres, C.A. and Cooper, J.K. Transmission of Electro-cardiograms to Computers. Military Medicine 129: 457-464. 1964.

14. Caceres, C.A. and Dreifus, L.S. Clinical Electrocardio-graphy and Computers. New York, N.Y. Academic Press. 1970.

15. Cady, L.D. et al A Method for Electrocardiogram Wave-Pattern Estimation. Circulation Research IX: 1078-1082. 1961.

16. Cooper, J.K. et al Role of a Digital Computer in a Diagnostic Center. Journal of the American Medical Association 193: 911-915. 1965.

17. DR8 Family Research Recorder, Electronics for Medicine Inc. White Plains, New York.

18. Ettinger, S.J. and Suter, P.F. Canine Cardiology. Philadel-phia, Pa. W.B. Saunders Company. 1970.

19. Franke, E.K., Braunstein, J.R. and Zellner, D.C. Study of High Frequency Components in Electrocardiogram by Power Spectrum Analysis. Circulation Research X: 870-879. 1962.

20. Goldman, M.J. Principles of Clinical Electrocardiography. Los Altos, California. Lange Medical Publications. 1964.

21. Graybiel, A. et al Analysis of the Electrocardiograms Obtained from 1000 Young Aviators. American Heart Journal 27: 524-549. 1944.

22. Guyton, A.C. Textbook of Medical Physiology, Philadelphia, Pa., W.B. Saunders Company. 1968.

23. Model 3960 Instrumentation Tape Recorder, Hewlett-Packard. Palo Alto, California.

24. Kimura, E., Mibukura, Y., and Miura, S. Statistical Diagno-sis of Electrocardiogram by Theorem of Bayes. A Preliminary Report. Japanese Heart Journal 4: 469-488. 1963.

25. Langner, P.H. and Geselowitz, D.B. Characteristics of the Frequency Spectrum in the Normal Electrocardiogram and in Subjects Following Myocardial Infarction. Circulation Research VIII: 577-584. 1960.

26. Martinek, G.C., Yeh, G.C.K., and Carnine, R. A New System for Electrocardiographic Recording, Analysis and Diagnosis. 112-116. 1959.

27. Martinez, P.E. Applications of Fourier and Bifore Analyses to Discrete Signals. Master's Report. Kansas State Univer-sity. Manhattan, Kansas. 1970.

28. Miyahara, H. et al   Cardiac Arrythmia Diagnosis by Digital Computer. Considerations Related to the Temporal Distribution of P and R Waves. Computers and Biomedical Research 1: 277-300. 1968.

29. Okajima, M. et al   Computer Pattern Recognition Techniques: Some Results with Real Electrocardiographic Data. IEEE Transactions on Biomedical Electronics 10: 106-114. 1963.

30. Pipberger, H.V. Use of Digital Computers in Analyzing Electrocardiographic Data. Grace Hospital Bulletin 41: 72-83. 1964.

31. Pipberger, H.V. et al   Digital Computer Analysis of the Normal and Abnormal Electrocardiogram. Progress in Cardiovascular Diseases 5: 378-392. 1963.

32. Pordy, L. et al   Computer Diagnosis of Electrocardiograms. IV. A Computer Program for Contour Analysis with Clinical Results of Rhythm and Contour Interpretation. Computers and Biomedical Research 1: 498-433. 1968.

33. Reikli, A.E. et al   Computer Analysis of Electrocardiographic Measurements. Circulation XXIV: 643-649. 1961.

34. Scher, A.M. and Young, A.C. Frequency Analysis of the Electrocardiogram. Circulation Research VIII: 344-346. 1960.

35. Schwan, H.P. Biological Engineering. New York, N.Y. McGraw-Hill Book Company. 1969.

36. Stallman, F.W. and Pipberger, H.V. Automatic Recognition of Electrocardiographic Waves by Digital Computer. Circulation Research IX: 1138-1143. 1961.

37. Steinberg, C.A. et al   Pattern Recognition in the Clinical Electrocardiogram. IRE Transactions on Bio-Medical Electronics 9: 23-30. 1962.

38. Taber, C.W. Taber's Cyclopedic Medical Dictionary. Philadelphia, Pa. F.A. Davis Company. 1962.

39. Thompson, N.P. Fourier Analysis of the Electrocardiographic Function. American Journal of Medical Electronics 1: 299-307. 1962.

40. Wartak, J. Computers in Electrocardiography. Springfield, Ill. Charles C. Thomas Publisher. 1970.

41. Whiteman, J.R. et al   Automation of Electrocardiographic Diagnostic Criteria. Journal of the American Medical Association 200: 932-938. 1967.

42. Winter, D.A. and Trenholm, B.G. Reliable Triggering for Exercise Electrocardiograms. IEEE Transactions on Bio-medical Engineering BME 16: 75-79. 1969.

43. _____ The American College Dictionary. New York, N.Y. Random House, 1959.

ACKNOWLEDGEMENTS

I wish to thank all those who throughout the course of this endeavor gave me help and encouragement. In particular, I would like to thank my advisory committee: Dr. Nasir Ahmed, Dr. Richard Gallagher and Dr. Frederick Rohles for their help and assistance in the carrying out of this project and for their encouragement which seemed to have been offered when most needed. I would also like to express my appreciation to Dr. Stanley Harris for his assistance in collecting and interpreting the physiological data which was the basis of this endeavor. Gratitude is also expressed for the financial support received through the National Institutes of Health Grant TOI UI 01050-01.

Finally, I would like to thank my family, my wife Kathy and my son Andrew for their understanding and encouragement during the course of my studies.

APPENDICES

APPENDIX I

Program for computation of the Bifore Power Spectrum

APPENDIX II

Program for least square error classification

APPENDIX III

Bifore or Hadamard Transform

```
C
//
//

      WRITE (6,9) (E(I,J),J=1,M)
      FORMAT(...)
   30 WRITE (6,7) (A(I,J),J=1,M)
   40 WRITE (6,6) (E(I,J),J=1,M)
      CALL ADD T(B,A,M)
   50 WRITE (6,8) (E(I,J),J=1,M)
   60 FORMAT(...)
      LL=1
      S=1
  220 K=0
      L=0
      S=1
  140 PSP=0.0
      DO 150 I=1,M
      IF(I.LE.LL) GO TO  230
      DO 145 J=1,N
      IF (J.LE.LL) GO TO 15  -5
      PSP=PSP+A(I,J)*X
  145 CONTINUE
  150 CONTINUE
      K=K+1
      B(K)=PSP
      L=VS
      S=S+VS
      IF(VS.LE.0) GO TO 16 24
      WRITE(3,A)(B(I),I=1,K)
  165 FORMAT(///(A,FF  ))
      LL=VS
      VS=2*VS
      IF(VS.LE.0) GO TO 16  12
      KP=KP+1
      IF(KP.LE.N)GO TO 15
      STOP
      END
      SUBROUTINE ADJST (A,  ,A)
      DIMENSION (A2,20),X(R )
      DO 60 I=1,N
      DO 60 J=1,N
   60 X(J)=A(I,J)
      CALL LEFT (X, )
   65 A(I,J)=X(J)
      DO 70 I=1,N
   70 X(I)=A(I,J)
      CALL LEFT (X, )
      X(J,J)=X(I)
```

```
      SUBROUTINE SHFT (ITEM,X)
      DIMENSION ITEM(50),X(32),Y(32)
   25 I=ISAC
      I=ITEM+NUM
   31 ITEM=ITEM/2
      IF (ITEM.EQ.0) GO TO 32
      ITEM=ITEM+1
      GO TO 31
   32 CONTINUE
      DO 40 M=1,ITEM
      IF (M.EQ.1) ALPF=1
      IF (M.NE.1) ALPF=ALPF*NP*Z
      NRUM=IUM/ALPH
      N=NRUM*ALN/2
      DO 40 NP=1,NLMF
      IB = (NP-2) * PALM
      IF NP=2,NNLMB
      N*NP21 = N(NP2 + PP2 + IB
      IE=A =1 + NPZ
      Y(IPA)=X(IPA)+X(NPALPZ1)
      Y(NPZ21)=X(IPA)-X(NPALPZ2)
   40 CONTINUE
      DO 70 I=1,NLP
   70 X(I) =Y(I)
   90 CONTINUE
      DO 120 I=.,NLP
      Y(I1)=Y(I1)/ALP
  120 X(I1)=Y(I1)
      RETURN
      END
```

```
C     LEAST SQUARE ERROR CLASSIFIER PROGRAM
C     N IS THE NUMBER OF SAMPLES IN EACH CLASS
C     L IS THE NUMBER OF COMPONENTS
      DIMENSION VX1(2,5),VX2(2,5),VX3(2,5),VX(2,5),YA(5,5),Y(5)
      DIMENSION XX1N(5,5),XINC(5,5),CF(5,5)
      DIMENSION XX1(5,5),XX2(5,5),XX3(5,5),XX(5,5),C(5,5),D(10,10)
      DIMENSION XA1(5,16),XA2(5,16),XA3(5,16),V(5,2),A(2,5),B(10,10)
      N=10
      L=4
      M=L+1
    1 FORMAT(10F8.2)
    2 FORMAT(10X,*XXIN(*,I1,*,*)=*,E12.5)
    3 FORMAT(/9X,* INVERSE MATRIX XXIN*,/)
    4 FORMAT(10X,*VX(*,I1,*,I1,*)=*,E12.5)
    6 FORMAT(10X,*A(*,I1,*,*,I1,*)=*,E12.5)
    8 FORMAT(2I4,C)
   11 FORMAT(2F7.3)
   12 FORMAT(10X,*XA1(*,I1,*,I2,*)=*,F4.1,4X,*XA2(*,I1,*,*,I2,*)=*,
     1F4.1)
   16 FORMAT (/9X*CONFUSION MATRIX*,/)
   17 FORMAT (11X,*CF(*,I1,*,*,I1,*)=*,I2)
   21 FORMAT(I2,1X,5(E12.5,2X))
      READ(5,1) ((XA1(I,J),J=1,N),I=1,M)
      READ(5,1) ((XA2(I,J),J=1,N),I=1,M)
      READ(5,1) ((V(I,J),J=1,2),I=1,2)
      DO 13 I=1,M
   13 WRITE (6,12)  (I,J,XA1(I,J),I,J,XA2(I,J),J=1,N)
      DO 1C I=1,M
      DO 1C K=1,M
      XX1(I,K)=C.0
      XX2(I,K)=C.0
      XX3(I,K)=C.0
      DO 15 J=1,N
      XX1(I,K)=XX1(I,K)+XA1(I,J)*XA1(K,J)+XY1(I,K)
   15 XX2(I,K)=XX2(I,K)+XA2(I,J)*XA2(K,J)+XY2(I,K)
   1C XX(I,K)=(XX1(I,K)+XX2(I,K))/(2*N)
      WRITE (6,6)
      WRITE(6,2) ((I,K,XX(I,K),K=1,M),I=1,M)
      CALL INVERS(XX,5)
      WRITE(6,3)
      WRITE (6,2) ((I,K,XX(I,K),K=1,M),I=1,M)
C     CONTINUE
      DO 20 I=1,2
      DO 2C J=1,M
      VX1(I,J)=C.0
      VX2(I,J)=C.0
      DO 25 K=1,N
      VX1(I,J)=VX1(I,J)+X*(I,K)+VX1(I,J)
   25 VX2(I,J)=VX2(I,J)+XA2(I,K)+VX2(I,J)
   2C VX(I,J)=(VX1(I,J)+VX2(I,J))/(2*N)
      WRITE(6,4) ((I,K,VX(I,K),K=1,M),I=1,2)
      DO 30 I=1,2
      DO 30 J=1,M
      A(I,J)=C.0
      DO 30 K=1,M
   30 A(I,J)=VX(I,K)*XX(K,J)+A(I,J)
      WRITE (6,6) ((I,K,A(I,K),K=1,M),I=1,2)
```

```
      DO 35 I=1,2
      DO 35 J=1,N
      C(I,J)=0.0
      DO 35 K=1,2
   35 C(I,J)=V(I,K)*A(K,J)+C(I,J)
      WRITE(6,9) ((I,K,C(I,K),K=1,N),I=1,2)
      DO 47 I=1,2
      DO 47 J=1,2
   47 CF(I,J)=0.0
      WRITE(6,8)
      DO 55 J=1,N
      DO 50 K=1,N
      X2(K,1)=X*A1(K,J)
      X1(K,2)=X*A2(K,J)
      DO 41 L=1,2
      DO 41 I=1,2
      C(I,L)=0.0
      DO 50 K=1,N
   50 C(I,L)=C(I,K)*XA(K,L)+C(I,L)
   41 WRITE (6,21) L,(C(I,L),I=1,2)
      DO 54 L=1,2
      LS=1
      CRT=C(L,L)
      DO 52 I=1,2
      IF (CRT.LT.C(I,L)) GO TO 52
      GO TO 53
   52 LS=I
      CPT=C(I,L)
   53 CF(LS,L)=CF(LS,L)+1
   54 CONTINUE
      WRITE(6,10)
      WRITE(6,17)  ((I,K,CF(I,K),K=1,2),I=1,2)
      STOP
      END
      SUBROUTINE INVERS(R,N)
      IMPLICIT REAL*8(A,C,G,F,C)
      DIMENSION A(5,5),G(5),F(5),R(5,5)
      DO 10 I=1,N
      DO 10 J=1,N
   10 A(I,J)=DBLE(R(I,J))
      NN=N-1
      Z(1,1)=1.0/A(1,1)
      DO 210 M=1,NN
      K=M+1
  250 DO 200 I=1,M
      G(I)=0.0
      DO 240 J=1,M
  240 C(I)=C(I)+A(I,J)*Z(J,K)
      DO 270 I=1,M
  270 G=G+A(K,I)*Z(I,1)
      G=-G+A(K,K)
      DO 200 J=1,M
  200 Z(I,1)=-Z(I,J)*G(J,1)
      Z(K,1)=1.0/G
      DO 200 I=1,N
```

```
100  F(J)=F(J)+A(K,I)*A(I,J)
     DO 200 J=1,N
200  A(K,J)=F(J)*A(K,K)
     DO 210 I=1,M
     DO 210 J=1,M
210  F(I,J)=C(I,J)-G(I)*A(K,J)
     DO 15 I=1,N
     DO 15 J=1,N
15   F(I,J)=S*GL(A(I,J))
     RETURN
     END
```

BIFORE or Hadamard Transform

N. AHMED, Member, IEEE
Department of Electrical Engineering
Kansas State University
Manhattan, Kans.

K. R. RAO, Member, IEEE
Department of Electrical Engineering
University of Texas at Arlington
Arlington, Tex.

L. ABDUSSATTAR, Student Member, IEEE
Department of Electrical Engineering
Kansas State University
Manhattan, Kans.

Abstract

BIFORE or Hadamard transform[1] is defined and several of its properties developed. BIFORE power and phase spectra are developed and their frequency–sequency composition is explored. Using matrix partitioning, fast algorithms for efficient computation of BIFORE coefficients power and phase spectra are developed. Multidimensional BIFORE transform is defined and a physical interpretation of its power spectrum is presented. Advantages and as well the limitations of the BIFORE transform in its application in information processing are cited.

[1] Also called Walsh–Hadamard transform.

Introduction

The notion of binary Fourier representation (BIFORE) was introduced by Ohnsorg [1]. BIFORE resembles the Fourier harmonic analysis in both geometrical and analytical characteristics. While the Fourier bases are sinusoids with harmonic frequencies, the BIFORE bases are Walsh functions. Since the Walsh functions are square waves, they take only two values, namely, $+1$ or -1. Thus, in the case of finite systems, these square waves are represented by binary n-tuples. The simplicity of square waves or binary n-tuples relative to sinusoids or sampled sinusoids permits relatively easy information processing in several applications which include signal representation and classification [2], image coding [3], spectral analysis of digital systems [4], speech processing [5], and sequency analysis and synthesis of voice signals [6]. Since only real number operations are involved, BIFORE transform (BT) can save additional computer time. Other advantages are possibly data compression, tolerance to channel errors, and reduced bandwidth transmission [3].

Walsh Functions

Walsh functions [7] are best introduced by referring to the following Fourier sinusoids.

$$U_0(t) = 1$$
$$U_{m,1}(t) = \cos(2\pi mt)$$
$$U_{m,2}(t) = \sin(2\pi mt), \qquad m = 1, 2, 3, \cdots \qquad (1)$$

The first five of the Fourier sinusoids are shown in Fig. 1 over the interval (0, 1). The corresponding Walsh functions $\{\psi_m(t)\}$ are shown in Fig. 2. Superimposition of these figures leads to the fact that:

1) $\psi_0(t) = U_0(t)$;
2) the zero crossings of the remaining pairs of pictured functions are identical.

This seems to indicate that the Walsh functions are an infinitely clipped version of the sinusoids. In general this is not the case, as the sign changes are not equidistant (Fig. 3). The total number of zero crossings of Walsh functions and corresponding sinusoids, however, are the same. Walsh functions can be generated recursively, are orthogonal, and form a closed set [7]–[9]. Signal analysis and synthesis can be carried out by expanding functions in Walsh series [6]. An expository article on applications of Walsh function has appeared recently [11].

Hadamard Matrices

Sampling of the Walsh functions shown in Fig. 3 at 2^3 equally spaced sample points $t_1, t_2, \cdots, t_8$ in (0, 1) results in an 8×8 array of $+1$'s and -1's. As each sample represents a constant section of the Walsh function, the information content is preserved. The rows of any array obtained by this method can be rearranged to form a particular matrix of

THIS BOOK WAS BOUND WITH PAGES 72 – 80 MARKED AS PAGES 226 – 234.

THIS IS AS RECEIVED FROM CUSTOMER.

Fig. 1.   Fourier harmonics.

Fig. 2.   Walsh functions.
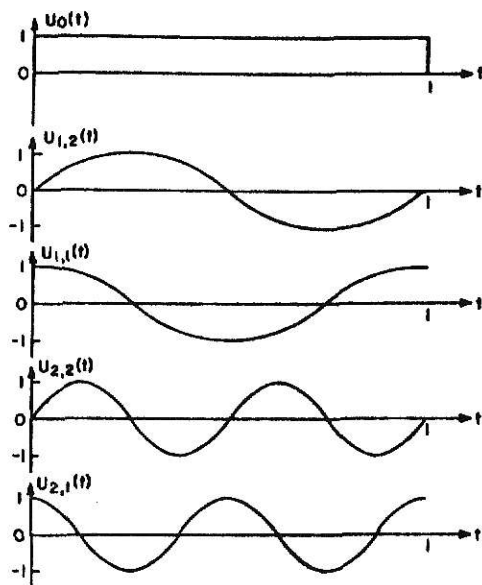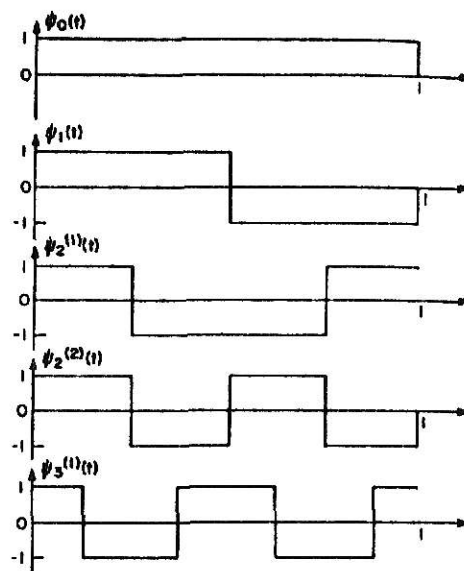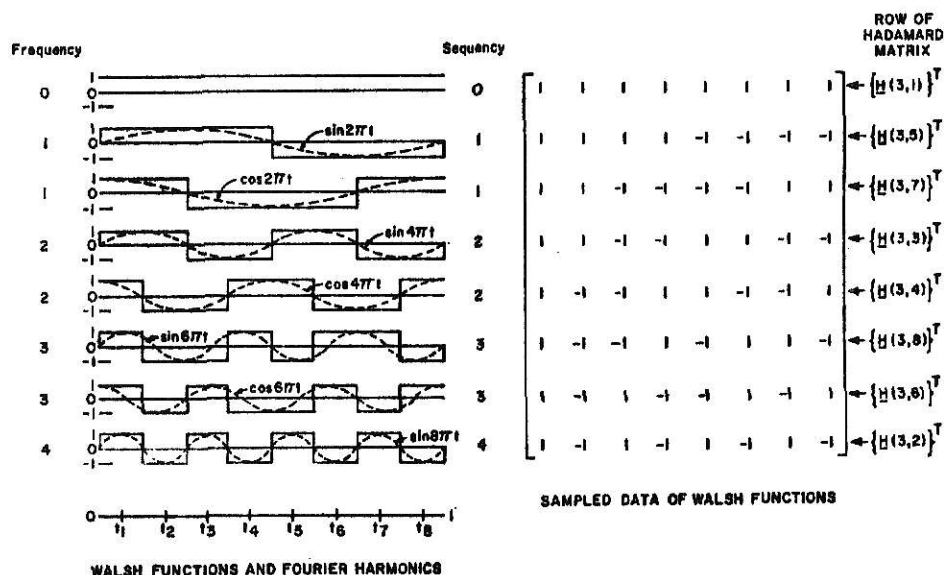

WALSH FUNCTIONS AND FOURIER HARMONICS

SAMPLED DATA OF WALSH FUNCTIONS

Fig. 3.   Fourier harmonics, Walsh functions, and Hadamard matrices for $n = 8$.

the type studied by Hadamard [12]. One such rearrangement is

$$[H(3)] = \begin{bmatrix} 1 & 1 & 1 & 1 & 1 & 1 & 1 & 1 \\ 1 & -1 & 1 & -1 & 1 & -1 & 1 & -1 \\ 1 & 1 & -1 & -1 & 1 & 1 & -1 & -1 \\ 1 & -1 & -1 & 1 & 1 & -1 & -1 & 1 \\ 1 & 1 & 1 & 1 & -1 & -1 & -1 & -1 \\ 1 & -1 & 1 & -1 & -1 & 1 & -1 & 1 \\ 1 & 1 & -1 & -1 & -1 & -1 & 1 & 1 \\ 1 & -1 & -1 & 1 & -1 & 1 & 1 & -1 \end{bmatrix} \quad (2)$$

where $[H(3)]$ is a $2^3 \times 2^3$ Hadamard matrix.

Thus, the periodic sampling of Walsh functions yield after rearrangment of the rows, Hadamard matrices whic can be recursively generated as follows:

$$[H(0)] = [1]$$

$$[H(k+1)] = \begin{bmatrix} [H(k)] & | & [H(k)] \\ ----- & | & ----- \\ [H(k)] & | & -[H(k)] \end{bmatrix},$$

$$k = 0, 1, 2, \cdots, g; \quad g = \log_2 n. \quad ($$

If $\{H(g, l)\}$, $l = 1, 2, \cdots, n$, $g = \log_2 n$, denotes the l column of $[H(g)]$, then its rows $\{H(g, l)\}^T$ serve as a bas set in the finite dimensional vector space of dimension

These matrices possess transform properties since $[H(g)]$ is both symmetric and orthogonal, i.e.,

$$[H(g)]^T[H(g)] = n[I(g)]$$

where $[I(g)]$ is the $n \times n$ identity matrix.

BIFORE or Hadamard Transform

BIFORE or Hadamard transform (BT or HT) of an n-periodic sequence $\{x(k)\} = \{x(0), x(1), \cdots, x(n-1)\}$ is defined as

$$\{B_z(g)\} = \frac{1}{n}[H(g)]\{x(g)\} \qquad (4)$$

where $\{x(g)\}^T = \{x(0)x(1) \cdots x(n-1)\}$ is the vector representation of the sequence $\{x(k)\}$ and $\{B_z(g)\}^T = \{B_z(0)B_z(1) \cdots B_z(n-1)\}$, the $B_z(\ )$ being the BT coefficients.

The signal can be recovered uniquely from the inverse BIFORE transform (IBT), i.e.,

$$\{x(g)\} = [H(g)]\{B_z(g)\}. \qquad (5)$$

Fast BIFORE Transform (FBT)

Using matrix factoring [13] or matrix partitioning [14], algorithms for fast and efficient computation of BT can be developed. Similar techniques are applicable to discrete Fourier and other orthogonal transforms [13]–[17]. As an example, for $n=8$, (4) can be expressed in matrix form as follows:
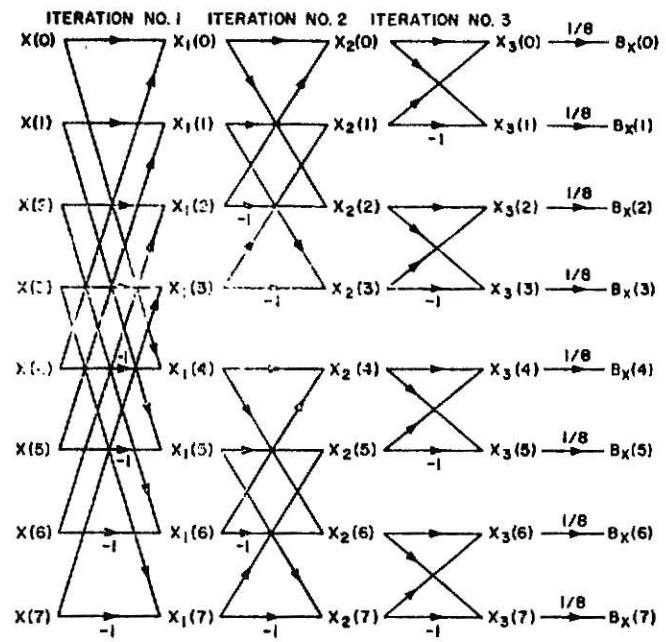

Fig. 4. Signal flow graph illustrating the computation of BT coefficients for $n = 8$.

1) The total number of iterations is given by $g = \log_2 n$. Thus, if r is an iteration index, then $r = 1, 2, \cdots, g$.

2) The rth iteration results in 2^{r-1} groups with $n/2^{r-1}$ members in each group. Half the members in each group are associated with an addition operation while the remaining half are associated with a subtraction operation.

3) The total number of arithmetic operations to compute

$$
\begin{Bmatrix} B_z(0) \\ B_z(1) \\ B_z(2) \\ B_z(3) \\ \hline B_z(4) \\ B_z(5) \\ B_z(6) \\ B_z(7) \end{Bmatrix} = \frac{1}{8}
\left[
\begin{array}{cc|c|cc}
\begin{pmatrix} 1 & 1 \\ 1 & -1 \end{pmatrix} & & 1 & \begin{pmatrix} 1 & 1 \\ 1 & -1 \end{pmatrix} & \begin{pmatrix} 1 & 1 \\ 1 & -1 \end{pmatrix} \\
\end{array}
\right]
\begin{Bmatrix} x(0) \\ x(1) \\ x(2) \\ x(3) \\ \hline x(4) \\ x(5) \\ x(6) \\ x(7) \end{Bmatrix}. \qquad (6)
$$

The structure of (6) suggests repeated applications of matrix partitioning, and the related sequence of computations is shown in the signal flow graph in Fig. 4. Apart from the $\frac{1}{8}$ multiplier, the total number of arithmetic operations (real additions and subtractions) required for computing the BT is $8 \times 3 = 24$.

Generalizations

The generalizations pertinent to the FBT are straightforward. The overall structure of the signal flow graph for any n is similar to that of Fig. 4. For the fast algorithm the following observations can be made.

all the transform coefficients is approximately $n \log_2 n$, compared to n^2 as implied by (4).

4) The algorithm can also be used to compute the IBT by merely omitting the constant multiplier $1/n$.

BIFORE Power Spectrum [18]

To entertain the idea of a BIFORE power spectrum, Parseval's theorem is developed. The transpose of (4) yields

$$\{B_z(g)\}^T = \frac{1}{n}\{x(g)\}^T[H(g)]^T. \qquad (7)$$

From (4) and (7) it follows that

$$\{B_x(g)\}^T \{B_x(g)\} = \frac{1}{n^2} \{x(g)\}^T [H(g)]^T [H(g)] \{x(g)\},$$

$$\{B_x(g)\}^T \{B_x(g)\} = \frac{1}{n} \{x(g)\}^T \{x(g)\}, \qquad (8)$$

or

$$\frac{1}{n} \sum_{h=0}^{n-1} x^2(h) = \sum_{h=0}^{n-1} B_x^2(h). \qquad (9)$$

BT of $\{x^{(1)}(3)\}$ is

$$\{B_x^{(1)}(3)\} = \tfrac{1}{8}[H(3)][M(3)]\{x(3)\}. \qquad (12)$$

That is,

$$\{B_x^{(1)}(3)\} = [A(3)]\{B_x(3)\} \qquad (13)$$

where

$$[A(3)] = \tfrac{1}{8}[H(3)][M(3)][H(3)]. \qquad (14)$$

Evaluation of the shift matrix $[A(3)]$ in (14) results in

$$[A(3)] = \frac{1}{2}
\begin{bmatrix}
2 & 0 & & & & & & \\
0 & -2 & & & 0 & & \\
& & 0 & -2 & & & 0 & \\
0 & & 2 & 0 & & & & \\
& & & & 1 & -1 & -1 & -1 \\
& 0 & & & 1 & -1 & 1 & 1 \\
& & & & 1 & 1 & 1 & -1 \\
& & & & -1 & -1 & 1 & -1
\end{bmatrix}. \qquad (15)$$

Thus, if the sequence $\{x(k)\}$ represents the sampled values of a current or voltage signal $x(t)$ and a 1 Ω pure resistive load is assumed, then the left-hand side of (9) represents the average power dissipated. The summation on the right-hand side of (9) implies that the signal power is conserved in the transform domain. The set $\{B_x^2(k)\}$, however, does not represent the individual spectral points as it is not invariant to the shift of the sampled data.

Development of the Spectrum

The development of the power spectrum is best illustrated by considering the case when $n=8$. Let $\{x^{(l)}(k)\}$ denote $\{x(k)\}$ shifted to the left by l positions. That is,

$$\{x^{(l)}(3)\}^T = \{x(l) x(l+1) \cdots x(l-2) x(l-1)\},$$

$$l = 1, 2, \cdots, 7$$

which with $l=1$ yields

$$\{x^{(1)}(3)\} = [M(3)]\{x(3)\} \qquad (10)$$

where

$$[M(3)] =
\begin{bmatrix}
0 & 1 & 0 & 0 & 0 & 0 & 0 & 0 \\
0 & 0 & 1 & 0 & 0 & 0 & 0 & 0 \\
0 & 0 & 0 & 1 & 0 & 0 & 0 & 0 \\
0 & 0 & 0 & 0 & 1 & 0 & 0 & 0 \\
0 & 0 & 0 & 0 & 0 & 1 & 0 & 0 \\
0 & 0 & 0 & 0 & 0 & 0 & 1 & 0 \\
0 & 0 & 0 & 0 & 0 & 0 & 0 & 1 \\
1 & 0 & 0 & 0 & 0 & 0 & 0 & 0
\end{bmatrix}. \qquad (11)$$

Repetitive application of (14) yields

$$\{B_x^{(l)}(3)\} = [A(3)]^l \{B_x(3)\}, \qquad l = 1, 2, \cdots, 7. \qquad (16)$$

$[A(3)]$ is made up of square matrices of increasing order along the diagonal. From the "block diagonal" structure of $[A(3)]$ and (16), the following set of equations is obtained:

$$B_x^{(l)}(0) = B_x(0)$$

$$B_x^{(l)}(1) = (-1)^l B_x(1)$$

$$\begin{bmatrix} B_x^{(l)}(2) \\ B_x^{(l)}(3) \end{bmatrix} = [D(1)]^l \begin{bmatrix} B_x(2) \\ B_x(3) \end{bmatrix}$$

and

$$\begin{bmatrix} B_x^{(l)}(4) \\ B_x^{(l)}(5) \\ B_x^{(l)}(6) \\ B_x^{(l)}(7) \end{bmatrix} = \frac{1}{2^l} [D(2)]^l \begin{bmatrix} B_x(4) \\ B_x(5) \\ B_x(6) \\ B_x(7) \end{bmatrix} \qquad (17)$$

where

$$[D(1)] = \begin{bmatrix} 0 & -1 \\ 1 & 0 \end{bmatrix}$$

and

$$[D(2)] = \frac{1}{2}\begin{bmatrix}
1 & -1 & -1 & -1 \\
1 & -1 & 1 & 1 \\
1 & 1 & 1 & -1 \\
-1 & -1 & 1 & -1
\end{bmatrix} \qquad (18)$$

are orthogonal. That is, $[D(1)]^T[D(1)] = [I(1)]$ and $[D(2)]^T[D(2)] = [I(2)]$.

Equation (17) implies that

$$(B_x^{(l)}(k))^2 = B_x^2(k), \qquad k = 0, 1;$$

$$\sum_{k=2}^{3} (B_x^{(l)}(k))^2 = \sum_{k=2}^{3} B_x^2(k) \qquad (19)$$

and

$$\sum_{k=4}^{7} (B_x^{(l)}(k))^2 = \sum_{k=4}^{7} B_x^2(k), \qquad l = 1, 2, \cdots, 7.$$

The set of invariants defined in (19) represents the power spectrum. In general, denote this spectrum as follows:

$$P_0 = B_x^2(0)$$

$$P_s = \sum_{k=2^{s-1}}^{2^s-1} B_x^2(k), \qquad s = 1, 2, 3, \cdots, g. \qquad (20)$$

Fast Algorithm for Power Spectrum

By suitably modifying the FBT approach, the power spectrum can be computed without having to actually compute all the coefficients $B_x(k)$. The modification is best illustrated for the case when $n = 8$.

From the signal flow graph in Fig. 4, it follows that

$$B_x(0) = x_3(0)/8$$

$$B_x(1) = x_3(1)/8$$

$$\begin{bmatrix} B_x(2) \\ B_x(3) \end{bmatrix} = \tfrac{1}{8}[H(1)]\begin{bmatrix} x_2(2) \\ x_2(3) \end{bmatrix}$$

and

$$\begin{bmatrix} B_x(4) \\ B_x(5) \\ B_x(6) \\ B_x(7) \end{bmatrix} = \tfrac{1}{8}[H(2)]\begin{bmatrix} x_1(4) \\ x_1(5) \\ x_1(6) \\ x_1(7) \end{bmatrix}. \qquad (21)$$

As $[H(g)]$ is orthogonal, one can obtain from (21)

$$\sum_{k=2}^{3} B_x^2(k) = \frac{2}{8^2} \sum_{m=2}^{3} c_2^2(m)$$

and

$$\sum_{k=4}^{7} B_x^2(k) = \frac{4}{8^2} \sum_{m=4}^{7} x_1^2(m). \qquad (22)$$

The power spectrum then is

$$P_0 = \frac{1}{8^2} x_3^2(0)$$

$$P_1 = \frac{1}{8^2} x_3^2(1)$$

$$P_2 = \frac{2}{8^2} \sum_{m=2}^{3} x_2^2(m)$$

and

$$P_3 = \frac{2^2}{8^2} \sum_{m=4}^{7} x_1^2(m). \qquad (23)$$

The generalization of the above FBT modification to compute the power spectrum is straightforward as indicated below.

$$P_0 = x_0^2(0)/n^2$$

$$P_s = \frac{2^{s-1}}{n^2} \sum_{m=2^{s-1}}^{2^s-1} x_{g+1-s}^2(m), \qquad s = 1, 2, \cdots, g. \qquad (24)$$

The signal flow graph corresponding to (24) is shown in Fig. 5.

Physical Interpretation of the BIFORE Power Spectrum

BIFORE power spectrum has dual significance. The spectrum points P_s represent the average powers in a set of $(g+1)$ sequences. Each spectral point also represents the power content of a group of frequencies rather than that of a single frequency. The n-periodic sequence $\{x(k)\}$ can be decomposed into an $n/2$-periodic sequence $\{F_1(k)\}$ and an $n/2$-antiperiodic[2] sequence $\{G_1(k)\}$ as follows:

$$\{x(k)\} = \{F_1(k)\} + \{G_1(k)\}$$

where

$$\{F_1(k)\} = \frac{1}{2}\left\{x(k) + x\left(k + \frac{n}{2}\right)\right\}$$

and

$$\{G_1(k)\} = \frac{1}{2}\left\{x(k) - x\left(k + \frac{n}{2}\right)\right\}. \qquad (25)$$

$\{F_1(k)\}$ can be further decomposed into an $n/4$-periodic sequence $\{F_2(k)\}$ and an $n/4$-antiperiodic sequence $\{G_2(k)\}$, i.e., $F_1(k) = \{F_2(k)\} + \{G_2(k)\}$ where

$$\{F_2(k)\} = \frac{1}{2}\left\{F_1(k) + F_1\left(k + \frac{n}{4}\right)\right\}$$

and

$$\{G_2(k)\} = \frac{1}{2}\left\{F_1(k) - F_1\left(k + \frac{n}{4}\right)\right\}. \qquad (26)$$

Continuing this process, it follows that the given n-periodic sequence $\{x(k)\}$ can be decomposed into the following $(g+1)$ subsequences:

$$\{x(k)\} = \{F_g(k)\} + \{G_g(k)\} + \{G_{g-1}(k)\} + \cdots + \{G_1(k)\} \qquad (27)$$

where $\{F_g(k)\}$ is a 1-periodic sequence and $\{G_{g-r}(k)\}$ is a 2^r-antiperiodic sequence, $r = 0, 1, \cdots, (g-1)$.

This process of decomposition is illustrated in Fig. 6 for $N = 8$. Thus the sequence $\{x(k)\}$ can be decomposed to obtain

$$\{x(k)\} = \{F_3(k)\} + \{G_3(k)\} + \{G_2(k)\} + \{G_1(k)\} \qquad (28)$$

where $\{F_3(k)\}$ is 1-periodic, while $\{G_3(k)\}$, $\{G_2(k)\}$, and

---

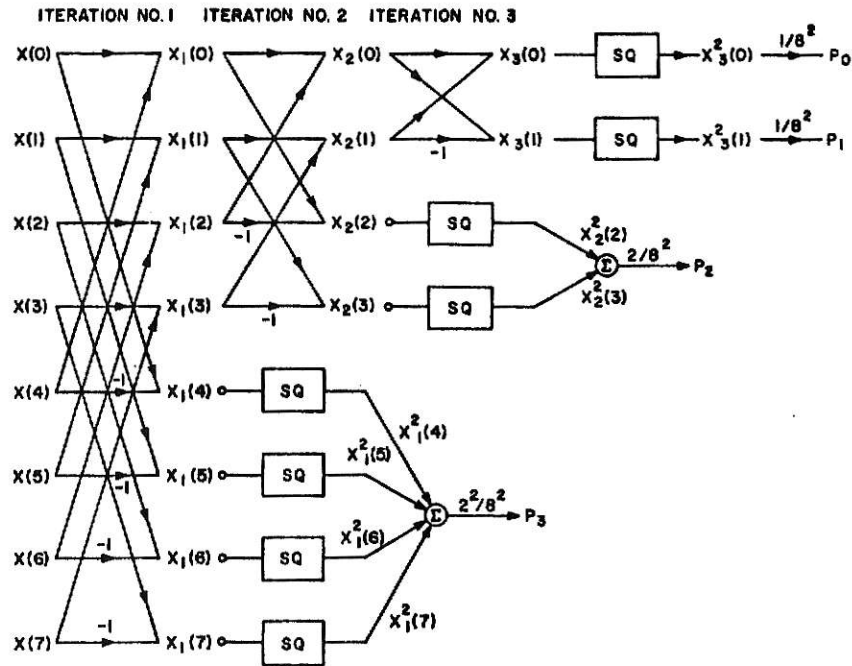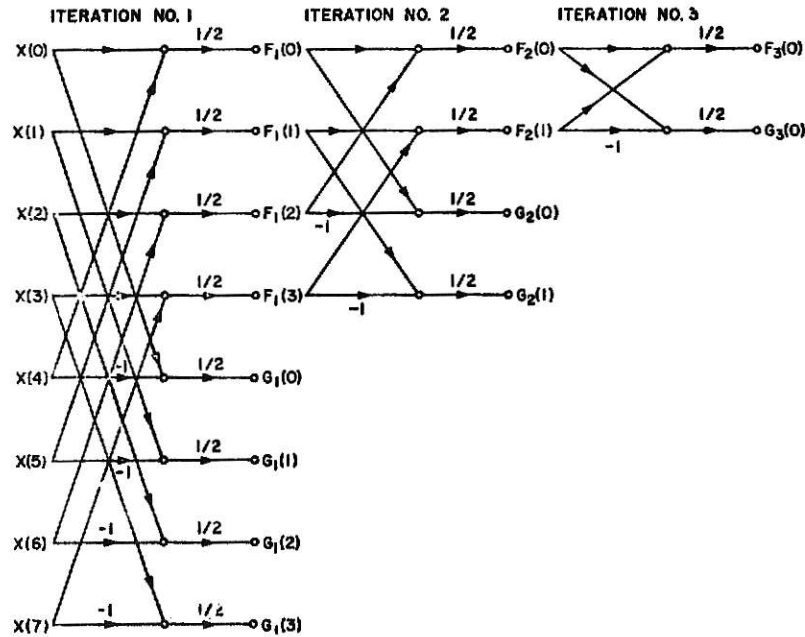[2] A sequence $\{x(k)\}$ is said to be M-antiperiodic if $x(m) = -x(M+m)$.

Fig. 5. Signal flow graph illustrating the computation of BT power spectrum.

Fig. 6. Flow graph illustrating the decomposition of $\{x(k)\}$ into subsequences.

$\{G_1(k)\}$ are respectively 1-, 2-, and 4-antiperiodic. Therefore, these sequences can be denoted by vectors as follows:

$$\{F_3(3)\}^T = \{b_x(0) \quad b_x(0) \quad b_x(0) \quad b_x(0) \quad b_x(0) \quad b_x(0) \quad b_x(0) \quad b_x(0)\}$$

$$\{G_3(3)\}^T = \{b_x(1) - b_x(1) \quad b_x(1) - b_x(1) \quad b_x(1) - b_x(1) \quad b_x(1) - b_x(1)\}$$

$$\{G_2(3)\}^T = \{b_x(2) \quad b_x(3) - b_x(2) - b_x(3) \quad b_x(2) \quad b_x(3) - b_x(2) - b_x(3)\}$$

$$\{G_1(3)\}^T = \{b_x(4) \quad b_x(5) \quad b_x(6) \quad b_x(7) - b_x(4) - b_x(5) - b_x(6) - b_x(7)\}$$

(29)

where the coefficients $b_x(k)$ will be expressed in terms of the BIFORE coefficients $B_x(k)$ at a later stage.

Inspection of the vectors in (29) shows that they are all mutually orthogonal and hence it follows that:

$$\|\{x(3)\}\|^2 = \|\{F_3(3)\}\|^2 + \|\{G_3(3)\}\|^2$$
$$+ \|\{G_2(3)\}\|^2 + \|\{G_1(3)\}\|^2 \quad (30)$$

where $\|\cdot\|$ represents the norm.

$$\|\{F_3(3)\}\|^2 = 8b_x^2(0), \quad \|\{G_3(3)\}\|^2 = 8b_x^2(1)$$

$$\|\{G_2(3)\}\|^2 = 4\sum_{k=2}^{3} b_x^2(k)$$

and

$$\|\{G_1(3)\}\|^2 = 2\sum_{k=4}^{7} b_x^2(k). \quad (31)$$

The average power of $\{x(k)\}$ is

$$P_{av} = \frac{1}{8}\sum_{m=0}^{7} x^2(m) = \frac{1}{8}\|\{x(3)\}\|^2.$$

From (30) and (31), there results

$$P_{av} = b_x^2(0) + b_x^2(1) + \frac{1}{2}\sum_{k=2}^{3} b_x^2(k)$$
$$+ \frac{1}{4}\sum_{k=4}^{7} b_x^2(k). \quad (32)$$

In terms of the decomposed sequences of $\{x(k)\}$, its BT can be expressed as

$$(33)$$

From (33) it follows that

$$B_x(0) = b_x(0), \quad B_x(1) = b_x(1);$$

$$\begin{bmatrix} B_x(2) \\ B_x(3) \end{bmatrix} = \tfrac{1}{2}[H(1)]\begin{bmatrix} b_x(2) \\ b_x(3) \end{bmatrix}$$

$$\begin{bmatrix} B_x(4) \\ B_x(5) \\ B_x(6) \\ B_x(7) \end{bmatrix} = \tfrac{1}{4}[H(2)]\begin{bmatrix} b_x(4) \\ b_x(5) \\ b_x(6) \\ b_x(7) \end{bmatrix}. \quad (34)$$

Since the matrices $[H(1)]$ and $[H(2)]$ are orthogonal, it follows that

TABLE I

Frequency–Sequency Composition of BIFORE Coefficients

BIFORE Component	Frequency	Sequency
$B_x(0)$	0	0
$B_x(1)$	4	4
$B_x(2)$	2	2
$B_x(3)$	2	2
$B_x(4)$	1	1
$B_x(5)$	3	3
$B_x(6)$	1	1
$B_x(7)$	3	3

$$\sum_{k=2}^{3} b_x^2(k) = 2\sum_{k=2}^{3} B_x^2(k)$$

and

$$\sum_{k=4}^{7} b_x^2(k) = 4\sum_{k=4}^{7} B_x^2(k).$$

Thus

$$P_{av} = B_x^2(0) + B_x^2(1) + \sum_{k=2}^{3} B_x^2(k) + \sum_{k=4}^{7} B_x^2(k)$$
$$= P_0 + P_1 + P_2 + P_3. \quad (35)$$

P_0 represents the average power in the 1-periodic sequence $\{F_3(k)\}$, while P_1, P_2, and P_3 represent the average powers in $\{G_3(k)\}$, $\{G_2(k)\}$, and $\{G_1(k)\}$ which are respectively 1-, 2-, and 4-antiperiodic. In general, P_r, $(r=1, 2, \cdots, g)$ represents the average power in $\{G_{g+1-r}(k)\}$.

An additional interpretation of the power spectrum is found in Table I which gives the frequency–sequency[3] structure of BIFORE transform derived from Fig. 3.

Denoting the frequency content of the spectral point P_s by $F(P_s)$, from Table I it follows that

$$F(P_0) = 0; \quad F(P_3) = 1, 3; \quad F(P_2) = 2; \quad F(P_1) = 4.$$

---

[3] "Sequency" is defined as one-half the average number of zero-crossings per unit time [11].
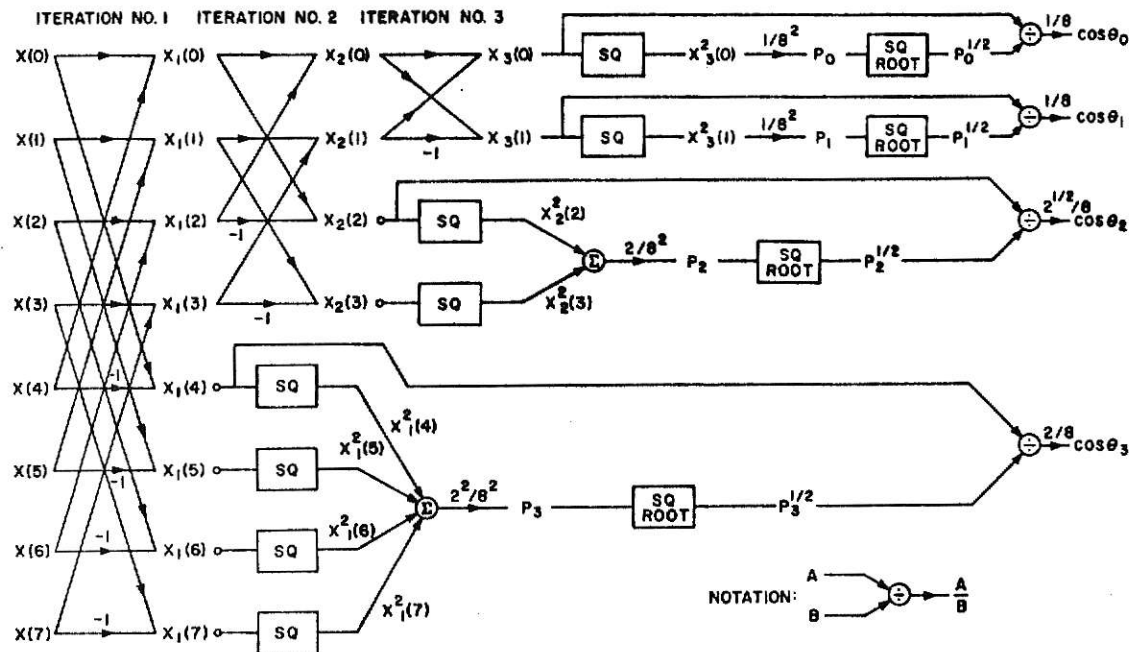
Fig. 7. Signal flow graph for computation of BIFORE power and phase spectra.

In general, then

$$F(P_0) = 0; \quad F(P_1) = n/2; \quad \text{and} \quad F(P_s) = 2^{g-s}(2k+1),$$

$$s = 2, 3, \cdots, g, \quad k = 0, 1, \cdots, (2^{s-2} - 1). \quad (36)$$

Clearly, each spectral point represents the power content of a group of frequencies rather than that of a single frequency as in the case of the Fourier transform. This frequency grouping, however, is not arbitrary. Each group contains a fundamental and the set of all odd harmonics relative to that fundamental. This corresponds to half-wave symmetry structure. Furthermore, there is a one-to-one correspondence between the $F(P_s)$ and the sequences $\{G_{g-r}(k)\}$.

BIFORE Phase Spectrum [19]

Analogous to the power spectrum, a phase spectrum of BT can be developed. Using the concepts of average power and phase angle, the phase spectrum is defined in multidimensional space in terms of a reference vector.

Average Power and Phase Angle

The average power P_{av} of and the angle θ between two n-dimensional vectors $\{x_1(g)\}$ and $\{x_2(g)\}$ are defined as

$$P_{av} = \frac{1}{n} \langle \{x_1(g)\}, \{x_2(g)\} \rangle$$

$$= \frac{1}{n} \| \{x_1(g)\} \| \, \| \{x_2(g)\} \| \cos \theta$$

$$\cos \theta = \frac{\langle \{x_1(g)\}, \{x_2(g)\} \rangle}{\| \{x_1(g)\} \| \, \| \{x_2(g)\} \|} \quad (37)$$

where the notation $\langle \cdot \rangle$ denotes the inner product.

Following the decomposition of $\{x(k)\}$ as in (27), the BIFORE phase spectrum can be developed [19] to yield

$$\cos \theta_0 = \frac{B_x(0)}{P_0^{1/2}}$$

$$\cos \theta_s = \frac{\sum_{k=2^{s-1}}^{2^s-1} B_x(k)}{2^{(s-1)/2} P_s^{1/2}}, \quad s = 1, 2, \cdots, g. \quad (38)$$

For $n=8$, (38) reduces to

$$\cos \theta_0 = \frac{B_x(0)}{P_0^{1/2}},$$

$$\cos \theta_1 = \frac{B_x(1)}{P_1^{1/2}},$$

$$\cos \theta_2 = \frac{\sum_{k=2}^{3} B_x(k)}{(2P_2)^{1/2}}$$

and

$$\cos \theta_3 = \frac{\sum_{k=4}^{7} B_x(k)}{(4P_3)^{1/2}} \cdot$$

This phase spectrum together with the power spectrum can be evaluated rapidly using the signal flow graph shown in Fig. 7. The phase spectrum is invariant to multiplication of the data sequence $\{x(k)\}$ by a real number but changes as the sequence is shifted. In fact it can be shown that the spectrum point $\cos \theta_s$ is 2^{s-1}-antiperiodic. Clearly, these properties are analogous to those of the DFT phase spec-

trum. However, the concept of phase is defined for groups of frequencies whose composition is the same as that of the power spectrum. Because of this frequency grouping and consequent data compression, the original sequence $\{x(k)\}$ cannot be recovered from the phase and power spectra as summarized in (20) and (38). This is in contrast to the DFT where the phase and power spectra are defined for individual frequencies and where the time signal can be reconstructed through them. Another phase spectrum based on sequency is developed by Boeswetter [6].

Multidimensional BT [20]

Analogous to DFT, BT can be generalized to any number of dimensions. The r-dimensional BT is defined as

$$B_f(u_1, u_2, \cdots, u_r)$$
$$= \prod_{i=1}^{r} \sum_{x_i=0}^{N_i-1} f(x_1, x_2, \cdots, x_r)(-1)^{\langle x, u \rangle} \quad (39)$$

where

$B_f(u_1, u_2, \cdots, u_r)$ is the transform coefficient.

$f(x_1, x_2, \cdots, x_r)$ is an input data point.

$u_i, x_i = 0, 1, 2, \cdots, N_i - 1, \qquad k_i = \log_2 N_i.$

$$\langle x, u \rangle = \sum_{j=1}^{r} \langle x_j, u_j \rangle.$$

$$\langle x_i, u_i \rangle = \sum_{m=0}^{k_i-1} x_i(m)u_i(m), \qquad i = 1, 2, \cdots, r.$$

The terms $u_i(m)$ and $x_i(m)$ are the binary representations of u_i and x_i, respectively, i.e.,

$$[u_i]_{\text{decimal}} = [u_i(k_i - 1), u_i(k_i - 2), \cdots,$$
$$u_i(1), u_i(0)]_{\text{binary}}.$$

$f(x_1, x_2, \cdots, x_r)$ can be recovered uniquely from the inverse BT, i.e.,

$$f(x_1, x_2, \cdots, x_r)$$
$$= \frac{1}{N} \prod_{i=1}^{r} \sum_{u_i=0}^{N_i-1} B_f(u_1, u_2, \cdots, u_r)(-1)^{\langle u, x \rangle} \quad (40)$$

where

$$N = \prod_{i=1}^{r} N_i.$$

Power Spectra

An extension of the power spectra of the 1-dimensional BT to the multidimensional case leads to the following:

$$P(z_1, z_2, \cdots, z_r) = \prod_{i=1}^{r} \sum_{u_i=2^{z_i}-1}^{2^{z_i}-1} B_f^2(u_1, u_2, \cdots, u_r) \quad (41)$$

where $z_i = 0, 1, 2, \cdots, k_i$. The total number of spectral points are $\prod_{i=1}^{r}(1+k_i)$. The frequency composition of the power spectra consists of all possible combinations of the groups of frequencies based on the odd-harmonic structure

(half-wave symmetry) in each dimension. For example, the frequency grouping in the ith dimension is

$$0$$

$$1, 3, 5, \cdots, \left(\frac{N_i}{2} - 1\right)$$

$$2, 6, 10, \cdots, \left(\frac{N_i}{2} - 2\right)$$

$$\cdots$$

$$\frac{N_i}{2}.$$

As an illustration, the frequency content for $N_1 = 8$, $N_2 = 16$, and $N_3 = 32$ consists of all possible combinations of the following groups.

N_1	N_2	N_3
0	0	0
1, 3	1, 3, 5, 7	1, 3, 5, 7, 9, 11, 13, 15
2	2, 6	2, 6, 10, 14
4	4	4, 12
	8	8
		16

The total number of spectral points is $\prod_{i=1}^{3}(1+k_i) = 120$. The power spectra defined in (41) is invariant to cyclic shift of the sampled data in any or all dimensions.

Properties

Other properties of the multidimensional BT can easily be derived. Some of these are listed as follows.

Parseval's Theorem:

$$\frac{1}{N} \prod_{i=1}^{r} \sum_{x_i=0}^{N_i-1} f^2(x_1, x_2, \cdots, x_r)$$
$$= \prod_{i=1}^{r} \sum_{u_i=0}^{N_i-1} B_f^2(u_1, u_2, \cdots, u_r). \quad (42)$$

Convolution: If

$$v(m_1, m_2, \cdots, m_r) = \frac{1}{N} \prod_{i=1}^{r} \sum_{x_i=0}^{N_i-1} f(x_1, x_2, \cdots, x_r)$$
$$\cdot h(m_1 - x_1, m_2 - x_2, \cdots, m_r - x_r) \quad (43)$$

where $m_i = 0, 1, 2, \cdots, N_i - 1$, then

$$\prod_{i=1}^{r} \sum_{u_i=2^{z_i}-1}^{2^{z_i}-1} B_v(u_1 u_2, \cdots, u_r)$$
$$= \prod_{i=1}^{r} \sum_{u_i=2^{z_i}-1}^{2^{z_i}-1} B_f(u_1, u_2, \cdots, u_r)B_h(u_1, u_2, \cdots, u_r). \quad (44)$$

Relationships similar to (44) are valid for cross correlation and autocorrelation.

Conclusions

The BIFORE transform and several of its properties are developed. These properties have been summarized and compared with those of DFT [21]. Fast algorithms for

aluation of BT, power and phase spectra are also developed. FBT can save computer time and result in reduced storage space as it requires about $n \log_2 n$ arithmetic operations to evaluate all the BT coefficients. Although the analysis in this paper has been restricted to real-valued sequences $x(k)$}, it can be easily extended to complex-valued sequences.

The BT has already found applications in several areas of information processing [11]. Greater utilization and exploitation of the BT, however, requires recognition of the ease and efficiency offered by the fast algorithms and development of methods for signal recovery from the spectra. This can lead to evolution of special purpose digital hardware tailored to specific application areas.

References

[1] F. R. Ohnsorg, "Binary Fourier representation," presented at the Spectrum Analysis Techniques Symp., Honeywell Res. Cen., Hopkins, Minn., Sept. 20–21, 1966.
[2] J. E. Whelchel, Jr., and D. F. Guinn, "The fast Fourier–Hadamard transform and its use in signal representation and classification," in Aerospace Electronics Conf., EASCON Rec., Sept. 1968, pp. 561–573.
[3] W. K. Pratt, J. Kane, and H. C. Andrews, "Hadamard transform image coding," Proc. IEEE, vol. 57, Jan. 1969, pp. 58–68.
[4] N. Ahmed and K. R. Rao, "Spectral analysis of linear digital systems using BIFORE," Electron. Lett., vol. 6, Jan. 22, 1970, pp. 43–44.
[5] G. S. Robinson and S. J. Campanella, "Digital sequency decomposition of voice signals," presented of the Walsh Function Symp., Naval Res. Lab., Washington, D. C., Mar. 31–Apr. 3, 1970.
[6] C. Boeswetter, "Analog sequency analysis and synthesis of voice signals," presented at the Walsh Function Symp., Naval Res. Lab., Washington, D. C., Mar. 31–Apr. 3, 1970.
[7] J. L. Walsh, "A closed set of normal orthogonal functions," Amer. J. Math., vol. 55, 1923, pp. 5–24.
[8] R. E. A. C. Paley, "On orthogonal matrices," J. Math. Phys., vol. 12, 1933, pp. 311–320.
[9] N. J. Fine, "On the Walsh functions," Trans. Amer. Math. Soc., vol. 65, 1949, pp. 372–414.
[10] K. W. Henderson, "Some notes on the Walsh function," IEEE Trans. Electron. Comput. (Corresp.), vol. EC-13, Feb. 1964, pp. 50–52.
[11] H. F. Harmuth, "Applications of Walsh functions in communications," IEEE Spectrum, vol. 6, Nov. 1969, pp. 82–91.
[12] J. Hadamard, "Resolution d'une question relative aux determinants," Bull. Sci. Math., ser. 2, vol. 17, 1893, pp. 240–246.
[13] H. C. Andrews and K. L. Caspari, "A generalized technique for spectral analysis," IEEE Trans. Comput., vol. C-19, Jan. 1970, pp. 16–25.
[14] N. Ahmed and S. M. Cheng, "On matrix partitioning and a class of algorithms," IEEE Trans. Educ., vol. E-13, Aug. 1970, pp. 103–105.
[15] E. O. Brigham and R. E. Morrow, "The fast Fourier transform," IEEE Spectrum, vol. 4, Dec. 1967, pp. 63–70.
[16] J. A. Glassman, "A generalization of the fast Fourier transform," IEEE Trans. Comput., vol. C-19, Feb. 1970, pp. 105–116.
[17] F. Theilheimer, "A matrix version of the fast Fourier transform," IEEE Trans. Audio Electroacoust., vol. AU-17, June 1969, pp. 158–161.
[18] N. Ahmed and K. R. Rao, "Convolution and correlation using binary Fourier representation," in Proc. 1st Annu. Houston Conf. Circuits, Systems and Computers, May 1969, pp. 182–191.
[19] N. Ahmed, K. R. Rao, and P. S. Fisher, "BIFORE Phase spectrum," presented at the 13th Midwest Symp. Circuit Theory, Univ. Minnesota, Minneapolis, Minn., May 7–8, 1970.
[20] N. Ahmed, R. M. Bates, and K. R. Rao, "Multidimensional BIFORE transform," Electron. Lett., vol. 6, Apr. 16, 1970, pp. 237–238.
[21] N. Ahmed and K. R. Rao, "Discrete Fourier and Hadamard transforms," Electron. Lett., Apr. 2, 1970, pp. 221–224.

APPLICATION OF A FREQUENCY APPROACH TO THE
CLASSIFICATION OF ELECTROCARDIOGRAPH SIGNALS

by

PAUL JOSEPH MILNE

B.S., Worcester Polytechnic Institute, 1967

———————————

AN ABSTRACT OF A MASTER'S THESIS

submitted in partial fulfillment of the

requirements for the degree

MASTER OF SCIENCE

Department of Electrical Engineering

KANSAS STATE UNIVERSITY
Manhattan, Kansas

1972

ABSTRACT

A plausible method for classification of electrocardio-
graphic data as coming from a normal or an abnormal subject using
the Bifore transform is demonstrated. Several types of ECG sig-
nals were obtained from research canines. These signals were
declared normal or abnormal by the veterinary cardiologist at
Kansas State University's Dykstra Veterinary Hospital. The
Bifore (Binary Fourier Representation) power spectrum* of these
signals was then obtained and four of these spectral points were
used to train a specific pattern classifier. The results of us-
ing the classifier show perfect classification of the normal and
abnormal signals from a given subject. In the case of signals
from a mixed population, a population consisting of samples from
all subjects, the classifier proved to be eighty-five per cent
correct.

The results suggest that the Bifore power spectrum could
prove useful in characterizing ECG's for the purpose of automatic
classification. Thus, recommendations for future work along
these lines are included.

---

*Also known as the Walsh-Hadamard power spectrum.